Fertilization unconventionally activates phospholipase C during the fast block to polyspermy in the African clawed frog, *Xenopus laevis*

by

Kayla M. Komondor

Bachelor of Science, Robert Morris University, 2019

Submitted to the Graduate Faculty of the

Dietrich School of Arts and Sciences in partial fulfillment

of the requirements for the degree of

Doctor of Philosophy

University of Pittsburgh

2024

UNIVERSITY OF PITTSBURGH

DIETRICH SCHOOL OF ARTS AND SCIENCES

This dissertation was presented

by

Kayla M. Komondor

It was defended on

March 8, 2024

and approved by

Jeffrey L. Brodsky, Avinoff Professor, Biological Sciences

Deborah L. Chapman, Professor, Biological Sciences

Gerry Hammond, Associate Professor, Cell Biology

Kevin D. Kohl, Associate Professor, Biological Sciences

Dissertation Director: Anne E. Carlson, Associate Professor, Biological Sciences

Fertilization unconventionally activates phospholipase C during the fast block to polyspermy in the African clawed frog, *Xenopus laevis*

Kayla M. Komondor, PhD

University of Pittsburgh, 2024

For most animals, fertilization by more than one sperm is lethal to a developing embryo. Accordingly, eggs use multiple mechanisms to keep additional sperm from entering the nascent zygote. One such mechanism, the fast block to polyspermy, is used by externally fertilizing animals and involves a change in the membrane potential of the egg from a negative resting potential to a positive fertilization potential. Sperm can bind to, but not enter, depolarized eggs. In frogs, fertilization opens the calcium-activated chloride channel TMEM16A, allowing an efflux of chloride ions that depolarize the egg's membrane. Currently, the signaling pathway by which fertilization opens TMEM16A is not yet known.

Using whole-cell recordings on *Xenopus laevis* eggs during fertilization, I have found that inhibiting phospholipase C (PLC) using the general PLC inhibitor U73122 abolishes the fast block depolarization, and polyspermic fertilization occurred. U73122 covalently modifies PLC, which enabled me to independently treat either egg or sperm prior to fertilization to identify which gamete provides the PLC. Whole-cell fertilization recordings with U73122 pretreated sperm showed typical fast block depolarizations and monospermic development, while pretreated eggs did not exhibit a depolarization and exhibited polyspermic development, indicating that the PLC necessary for the fast block is egg-derived. *X. laevis* eggs have three PLC subtypes (PLCγ1, PLCβ1, and PLCβ3). Each PLC subtype typically uses different activation methods: PLCγ1 is canonically activated by tyrosine phosphorylation, and PLCβ is typically activated through the $G\alpha_{q/11}$ subunit of G-protein coupled pathways. Inhibiting these methods of canonical activation revealed typical

depolarizations during whole-cell recordings and monospermic development. Together, these data reveal that the egg PLC during the fast block to polyspermy in *X. laevis* is activated by a novel signaling mechanism.

Table of Contents

Preface ..... **x**

List of Abbreviations ..... **xiii**

1.0 Introduction **1**

1.1 Fertilization **1**

1.1.1 History of fertilization research **1**

1.1.2 Introduction to sperm **2**

1.1.3 Introduction to eggs **3**

1.1.4 Mating in *X. laevis* **5**

1.1.5 Sperm and egg interaction **6**

1.1.6 Fertilization increases the cytoplasmic Ca^{2+} in the egg **7**

1.2 Polyspermy is embryonic lethal for most animals **7**

1.2.1 Polyspermy causes gross chromosomal abnormalities **8**

1.2.2 Slow block to polyspermy **8**

1.2.3 Fast block to polyspermy **9**

1.2.3.1 History of the fast block **9**

1.2.3.2 Many animals use the fast block to polyspermy **11**

1.2.3.3 Fast block mechanism **13**

1.3 Details of the fast block in *Xenopus laevis* **14**

1.3.1 Introduction to *X. laevis* as a model **14**

1.3.2 TMEM16A conducts the depolarizing current during the fast block **14**

1.3.3 The fast block is mediated by the production of IP_3 from PLC activation **16**

1.4 Phospholipase C 19

1.4.1 Background of PLCs 19

1.4.2 PLCδ and PLCη 21

1.4.3 PLCε 22

1.4.4 PLCγ 23

1.4.5 PLCβ 24

1.4.6 PLCζ 25

1.5 Summary of research goals 25

2.0 Methods 26

2.1 Reagents 26

2.2 Solutions 26

2.3 Animals 27

2.4 Collection of gametes 27

2.4.1 Fertilization-competent eggs 27

2.4.2 Sperm 28

2.4.3 Oocytes 28

2.5 Electrophysiology 28

2.5.1 Whole-cell recordings 29

2.5.2 Two-electrode voltage clamp (TEVC) recordings 29

2.6 Polyspermy Assay 30

2.7 Bioinformatics 30

2.8 Exogenous protein expression in *X. laevis* oocytes 30

2.9 Removal of egg jelly 31

2.10 Sample preparation and western blot 32

2.11 Quantification and statistical analyses 33

3.0 Results 34

3.1 Fertilization signals a depolarization in *X. laevis* eggs 34

3.2 PLC is required to signal a depolarization in *X. laevis* eggs during fertilization ... 36

3.3 An egg-derived PLC is responsible for evoking the fast block in *X. laevis* 38

3.4 *X. laevis* eggs have three PLC candidates for triggering the fast block 41

3.5 Tyrosine phosphorylation of PLCγ1 does not signal the fast block 42

3.6 $G\alpha_{11}$ activation of PLCβ is not required for the fast block in *X. laevis* 48

4.0 Discussion 54

4.1 Summary 54

4.2 The role of tyrosine phosphorylation in PLCγ activation is controversial 54

4.3 U73122 mechanism is controversial 56

4.4 Activation of PLCβ by other pathways in *X. laevis* eggs 57

5.0 Future Studies 58

5.1 Potential activation mechanisms of PLC during the fast block in *X. laevis* 58

5.2 How does depolarization of the egg membrane stop sperm entry? 59

6.0 Significance and Broader Implications 61

Appendix A Appendices and Supplemental Content 62

Appendix A.1 Tables 62

Bibliography 63

List of Figures

Figure 1: The fast block to polyspermy pathway in *X. laevis*. 18

Figure 2: PLC structures organized by isozyme. 20

Figure 3: Fertilization evokes a depolarization in *X. laevis*. 35

Figure 4: U73122 inhibits PLCs during the fast block to polyspermy in *X. laevis*. 37

Figure 5: An egg-derived PLC is activated during the fast block to polyspermy in *X. laevis*. 39

Figure 6: *X. laevis* eggs contain three PLC subtypes. 42

Figure 7: Tyrosine phosphorylation of PLCγ1 is not required for the fast block in *X. laevis*. 45

Figure 9: Fertilization did not trigger phosphorylation of Y776 of PLCγ1 in *X. laevis*. 47

Figure 10: Screening $G\alpha_{q/11}$ inhibitor efficacy in *X. laevis* oocytes. 50

Figure 11: Inhibiting PLCβ1/3 activation via $G\alpha_{11}$ did not alter the fast block to polyspermy in *X. laevis* eggs. 53

Preface

I would like to thank and acknowledge my dissertation committee for their support and advice throughout my studies at the University of Pittsburgh. My work has been supported through the T32 Training Program: Interinstitutional Program in Cell and Molecular Biology: A Graduate Training Path to Promote Traditional and Non-Traditional Professional Outcomes.

I must extend a huge thank you to past and present members of the Carlson Lab. I have been so fortunate that for the last five years, I have been able to wake up every day and know that I will get to do science with some of my favorite people. Wase, thank you for teaching me the ins and outs of the electrophysiology techniques we use in the lab, and for being the best lab partner I could have asked for during our shift work from the pandemic. Your support throughout my early career in the lab was monumental. Rachel, I could not have asked for a better support system, partner, or co-first author of our publication. Getting to know you as a scientist and friend has been incredibly insightful and deeply rewarding. Crystal and Jenny, watching both of you turn into two of the smartest, most independent scientists has been the highlight of my time in the lab. I cannot wait to see what you both do next. Thank you for being my rock for my last year in lab, especially leading into my dissertation defense. Joel, thank you for answering endless questions, somehow with more patience every time. Your help anytime I was stuck on an experiment or couldn't exactly get my math correct pushed me through to the finish line. And finally, I could not thank the lab without thanking Anne. You showed me not only the kind of science I was interested in, but also the kind of scientist I want to be. There is nothing you wouldn't do to see your students thrive and be successful, and I know that if I become even half of the mentor you are, I will be damn good at it.

I have been incredibly fortunate to have some of the greatest people in my life. My family has been my biggest support system. Gaga, thank you for supporting me through absolutely everything. There has not been an event that has been missed in all my 27 years (and believe me, there have been a lot of events). I am so grateful that you are not only my grandma, but also my best friend (XXOO). To my cousins who are more like my sisters, I truly don't know what I would do without you. You all mean the world to me, and I am so very lucky that we ended up choosing to be friends on top of being family. And to my brother, Cameron, thank you for your support, reality checks, and the occasional doubt (that was always nothing more than lighthearted sibling banter) that pushed me through.

From the friends I have from childhood, into undergrad, and then grad school, your love and support throughout not only these 5 years, but throughout all the different stages of my life, has been what has kept me going. There is not a single day that I don't sit back with awe at how fortunate I am to have each and every one of you in my life.

In the summer of 2023, I spent 6 weeks at Frontiers in Reproduction in Woods Hole, MA. I learned more from this course than I ever could have imagined, and I met some of my favorite people in my time there. I am still trying to decide if I learned more from the course itself, or more from each of the other FIRbees I met.

Finally, I would like to dedicate this dissertation to my parents. Throughout my undergraduate and grad school careers, we learned a lot together (i.e. FAFSA, loans, applications, buying books… you get it, the list goes on). I am so grateful that you heard me say something crazy like, "I want to go to school for five more years to get my Ph.D.," after undergrad and supported my decision, even after all of that. I often find myself saying that my parents are two of

the best people that I know, and I truly mean that. Thank you for teaching me how to be a strong, independent, and empathetic person. You both have always simply taught by example.

List of Abbreviations

BME: β-mercaptoethanol

DAG: diacylglycerol

DMSO: dimethyl sulfoxide

ECM: extracellular matrix

IP_3: inositol 1,4,5-trisphosphate

IP_3R: inositol 1,4,5-trisphosphate receptor

ER: endoplasmic reticulum

HSD: honestly significant difference (Tukey)

MR (/#): Modified Ringers solution (/dilution)

OHB: oocyte homogenization buffer

Opto-M1R: rhodopsin-muscarinic receptor type 1 chimera

PDGF/-R: platelet-derived growth factor/-receptor

PIP_2: phosphatidylinositol 4,5-bisphosphate

PIP_3: phosphatidylinositol 3,4,5-trisphosphate

PLC: phospholipase C

PLD: phospholipase D

SH2/3: Src-homology 2/3

TMEM16A: transmembrane 16A

VSP: voltage-sensing phosphatases

X. laevis: *Xenopus laevis*

1.0 Introduction

For most sexually reproducing animals, successful embryonic development requires that an egg is fertilized by only one sperm. In order to prevent fertilization by multiple sperm, a condition known as polyspermy, eggs have evolved different mechanisms to stop additional sperm from entering already fertilized eggs. These processes are called polyspermy blocks and are conserved in eggs from diverse animals. These polyspermy blocks take two forms, which have been named for their timing: the fast block occurs immediately after fertilization, whereas the slow block to polyspermy occurs minutes later. My dissertation aims to uncover the signaling events that trigger the fast block to polyspermy in eggs from the African clawed frog, *Xenopus laevis*.

1.1 Fertilization

1.1.1 History of fertilization research

Fertilization research can be traced back at least to 1677 when Dutch draper and microscopist Antonie van Leeuwenhoek first observed sperm. Leeuwenhoek used his homemade microscopes to examine his semen, where he identified the swimming, animal-like cells that he named "spermatozoon" – "sperma" meaning "seed" and "zoon" meaning "animal" (Puerta Suarez, du Plessis, & Cardona Maya, 2018). Leeuwenhoek noted that the sperm cells swam, and he speculated that they might have a role in reproduction. His findings were initially met with skepticism; however, his careful observations and detailed records eventually convinced the

scientific community of their existence. 100 years after Leeuwenhoek first observed sperm, the Italian priest and scientist Lazzaro Spallanzani performed the first successful artificial insemination. Spallanzani demonstrated that dressing male frogs in pants during mating events stopped embryonic development in frog eggs (Spallanzani, Bonnet, & Beddoes, 1789). Spallanzani also mixed frog eggs with semen acquired from the oilskin pants after mating, thereby establishing that male and female-derived material was required for successful fertilization and embryonic development. As he repeated the experiments, he made slight adjustments and eventually was able to replicate the fertilization events in several amphibian species, including salamanders, toads, and newts. He followed up on these findings in mammals, where he tracked a female poodle's ovulation cycle, injected semen into her uterus, and successfully performed the first artificial insemination for internal fertilizers, which gave rise to three healthy puppies (Penna, 2022). Much has been learned about fertilization since these critical, foundational experiments, and frogs remain key model organisms for fertilization research.

1.1.2 Introduction to sperm

Frog sperm, including sperm from *Xenopus laevis*, exhibit several characteristics that distinguish them from mammalian sperm, including their morphology, swimming behavior, their acrosome reaction, and ability to undergo chemotaxis (Tholl et al., 2011). Generally, frog sperm are smaller and have a simpler structure than mammalian sperm. The head of frog sperm is often more rounded and lacks the distinct acrosomal cap found in mammalian sperm. *X. laevis* sperm have a rigid corkscrew-like shape, a morphology that differs from the long and flexible tail of mammalian sperm that aids in their navigation through the viscous fluids of the female reproductive tract. The corkscrew-shaped sperm is observed in some species of frogs and other

amphibians but is not shared by all frog sperm. The flagellum in *X. laevis* sperm is responsible for motility but is particularly suited to the aquatic environment where these sperm fertilize. Sperm from frogs such as *X. laevis* are quiescent while in the testes and become active at mating when they move from the isotonic internal condition to the hypotonic condition of the environment when externally fertilizing the female's laid eggs. In frogs such as *X. laevis*, the sperm move from the testes through the Bidder's canal until they arrive in the cloaca, a cavity that allows for release from the reproductive and digestive tracts (Unsicker, Axelsson, Owman, & Svensson, 1975). Hypo-osmotic shock activates *X. laevis* sperm when they encounter the low salinity external environment of pond water, and this activation causes sperm swimming patterns to change, allowing for penetration of the jelly layer and then the membrane surrounding the eggs (Reinhart, Ridgway, & Chandler, 1998).

1.1.3 Introduction to eggs

Eggs, the largest nutrient-dense cells made by animals, are finely tuned for development (Alberts, 2002). For most animals, the egg contains the necessary components for the initial cell divisions until the maternal-to-zygotic transition occurs, which is when the maternal transcripts and proteins are cleared from the embryo, and activation of the zygotic genome takes place (Yang, Aguero, & King, 2015). *X. laevis* eggs contain the components necessary for the first 4,000 cell divisions as an embryo (Yang et al., 2015), which is thought to contribute to the large size of *X. laevis* eggs. Egg size also corresponds with the nutrient sources of the fetus. For example, humans have small eggs with minimal yolks because the growing fetus derives its nutrition from the mother through the placenta. Conversely, frogs, which rely on external fertilization and embryonic development, produce larger eggs with a substantial supply of yolk protein to nourish the

developing embryo (Alberts, 2002). The considerable size of *X. laevis* eggs not only benefits the frog reproduction strategy but also facilitates research, as their dimension allows for easy manipulation and experimentation in laboratory settings.

X. laevis eggs are surrounded by a sticky jelly coat that acts as both a protection mechanism and an adaptive trait to increase the likelihood of successful reproduction. The jelly gives the egg structural support while also giving the sperm a "landing pad" to stick to and facilitate fertilization. The stickiness of the jelly also enables the eggs to cluster and stop the clutch from floating free in the water where they could be subjected to predation. The jelly layer of the egg is enriched with components such as Ca^{2+} (Wozniak et al., 2017) and the chemoattractant, called allurin needed for successful fertilization in *X. laevis* (Burnett, Xiang, Bieber, & Chandler, 2008).

Eggs from most animals are surrounded by a tough extracellular matrix (ECM) comprised of a few glycoproteins that are thought to protect the egg and developing embryo. In frogs, the egg's ECM is called the vitelline envelope, whereas this structure is referred to as the zona pellucida in mammalian eggs and chorion in fish. Interestingly, the ECM's proteins are highly conserved from abalone to frogs to humans (Clark, Aagaard, & Swanson, 2006). Sperm can bind to the ECM, and this sperm-ECM binding is hypothesized to enable species-specific gamete recognition (Gilbert & Barresi, 2020). Additionally, this sperm-ECM binding helps to concentrate sperm around the egg, thereby increasing the efficiency of fertilization. This is especially important in aquatic environments, where frog sperm and eggs are released into the water, as it ensures that sperm remain close to the egg despite water currents and other dispersing forces. In *X. laevis*, two major glycoproteins, gp69 and gp64 (homologous to ZP2 and ZP3 in mammals), form the vitelline envelope (Tian, Gong, Thomsen, & Lennarz, 1997). During the slow block to polyspermy, the ECM and the plasma membrane separate from the cleavage of the structure that connects the two

layers, leading to embryo hatching during development (Grey, Wolf, & Hedrick, 1974). These structures of the egg are crucial for development and for fertilization that follows mating.

1.1.4 Mating in *X. laevis*

Mating in *X. laevis*, involves a unique courtship behavior where the male grasps the female in a mating embrace called amplexus. During this process, the female lays eggs while the male simultaneously releases sperm for external fertilization. This synchronization ensures successful reproduction and is a common practice among many amphibians. Although this mating system enables the gametes to mix immediately, this mating system also gives rise to obstacles to successful fertilization and embryonic development, including a high sperm-to-egg ratio. Unlike internally fertilizing animals where few sperm successfully travel to the egg (Coy, Garcia-Vazquez, Visconti, & Aviles, 2012), sperm from externally fertilizing animals do not have to traverse the anatomical maze of the female reproductive tract. It has been proposed that this excess of sperm relative to eggs is why the fast block is necessary (Gilbert, 2003).

Following mating, *X. laevis* sperm use chemotaxis to find the egg (Burnett, Sugiyama, Bieber, & Chandler, 2011; Burnett et al., 2008). Chemotaxis is a process where cells move toward a chemical gradient. In *X. laevis*, the jelly surrounding the egg contains allurin (Sugiyama et al., 2009), a potent chemoattractant that forms a concentration gradient (al-Anzi & Chandler, 1998). Allurin is a component of the egg jelly layer that is added during the egg's passage through the reproductive system, rather than released from the egg in a controlled cellular process (Xiang, Burnett, Rawls, Bieber, & Chandler, 2004). This chemical map drawn by allurin is crucial for ensuring that sperm find and fertilize eggs in the aquatic environment where they are released.

Although controversial, there is evidence progesterone released from the cells surrounding human eggs, is used for chemotaxis by human sperm (Teves et al., 2009).

1.1.5 Sperm and egg interaction

Fertilization involves the fusion of two cells, the sperm and the egg, an event that triggers new life and represents an active area of research where several fundamental questions remain unanswered. Sperm-egg binding is facilitated by proteins localized to the plasma membrane of each gamete. The sperm proteins Izumo1, SPACA6, and TMEM81 form a heterotrimer required for sperm-egg binding in vertebrates (Victoria E. Deneke et al., 2023). In contrast to the highly conserved sperm complex, the egg receptor is not well conserved. In mammals, this complex binds to the egg protein Juno, and to Bouncer in fish (Victoria E. Deneke et al., 2023). Interestingly, the sperm receptor in frog eggs remains elusive. To date, Izumo1 and Juno are the only known interacting proteins that are essential for fertilization in mammals (V. E. Deneke & Pauli, 2021).

Neither the process of sperm-egg fusion nor the proteins required for this fusion have been characterized for frogs or mammals. Previous research suggested that the fusion between sperm and egg in *X. laevis* was analogous to fertilization in fish and sea urchin where actin polymers from the egg were responsible for bringing the sperm into the egg (Limatola, Chun, & Santella, 2022). However, inhibition of actin polymerization during the *X. laevis* fertilization has shown that these protrusions are not necessary for *X. laevis* sperm-egg fusion at fertilization (Tembo et al., 2021).

1.1.6 Fertilization increases the cytoplasmic Ca^{2+} in the egg

Fertilization signals an elevation in the egg's cytoplasmic Ca^{2+}, a phenomenon that is conserved in nearly all animals and several plants (M. Whitaker, 2006). This intracellular Ca^{2+} signals the polyspermy blocks, initiates embryonic development, and regulates the early embryo's cell division and patterning process (M. Whitaker, 2006). In addition to its importance in activating the egg to prevent polyspermy, the increase in Ca^{2+} in *X. laevis* eggs at fertilization is also important for initiating embryonic development by triggering the exit of the condition of meiotic arrest that *X. laevis* eggs are in prior to fertilization (Tokmakov, Stefanov, Iwasaki, Sato, & Fukami, 2014). A review detailing the sources of calcium in egg activation of many external fertilizers hypothesized that Ca^{2+} is the main activation mechanism in the egg (L. F. Jaffe, 1983). In the years since this review, we have seen that Ca^{2+} is important for fertilization, polyspermy blocks, and development in nearly all sexual reproducers studied to date.

1.2 Polyspermy is embryonic lethal for most animals

Polyspermy, or fertilization of an egg by more than one sperm, is an obstacle to successful embryonic development for nearly all sexual reproducers. Interestingly, some animals require polyspermic fertilization to initiate development, like some birds, reptiles, and even some amphibians (Mizushima, 2017). For these animals, anywhere from 10 to hundreds of sperm trigger successful development. Like frogs, salamanders are amphibians, but salamanders use internal fertilization. Additionally, salamander eggs are noted to be inseminated by multiple sperm (Elinson, 1986). Polyspermy is lethal for nearly all animals, and fertilization by multiple sperm

leads to chromosomal abnormalities and dysregulation of cellular processes such as cell division and eventually leads to cell death (Elinson, 1986). Monospermic animals strictly regulate fertilization to ensure that only one sperm fertilizes the egg, employing various methods to prevent polyspermy.

1.2.1 Polyspermy causes gross chromosomal abnormalities

For most animals, embryos cannot survive the excess genetic material resulting from polyspermic fertilization. This causes dysregulation of DNA replication in the embryo, which leads to cell death, as the egg cannot maintain its cell cycle regulation with the excess nuclear content that comes with multiple sperm fertilizations (Skinner, 2018). Due to its catastrophic nature, eggs have developed methods to stop sperm from entering already fertilized eggs. Two of these commonly used polyspermy blocks are named for their relative timing: the fast and slow blocks to polyspermy.

1.2.2 Slow block to polyspermy

The slow block to polyspermy is a process observed in eggs from most sexually reproducing animals (Bianchi & Wright, 2016; Metz, 2012; Runft, Jaffe, & Mehlmann, 2002; Stricker, 1999; Wong & Wessel, 2006) and is initiated by a fertilization-signaled increase in the eggs' cytoplasmic Ca^{2+} levels. Docked at the plasma membrane of eggs from almost all sexual reproducers are secretory vesicles called cortical granules (Berg & Wessel, 1997; Liu, 2011; Wyrick, Nishihara, & Hedrick, 1974). Although the exact contents of the cortical granules remain an active area of research, it is known that there is a release of Zn^{2+} that occurs during this release,

known as a Zn^{2+} spark, that is conserved in external and internal fertilizers (Wozniak et al., 2020). The role of Zn^{2+} during the slow block is thought to play a direct role in incapacitating the sperm surrounding the egg to prevent supernumerary fertilization events. During the slow block, fertilization triggers the release of these cortical granules, the contents of which target the ECM and the plasma membrane, stop sperm from entering, and harden the structure of the ECM to protect the nascent zygote (Nishio et al., 2023; Wessel & Wong, 2009). This process is highly conserved. Once fertilization occurs, the membrane structure is modified, and proteins that sperm interact with are cleaved to prevent more sperm from entering.

1.2.3 Fast block to polyspermy

1.2.3.1 History of the fast block

The first description of polyspermy blocking mechanisms was published in 1919 by Ernest Everett Just, who reported a physical lifting of the membrane of sand dollar eggs following fertilization (Just, 1919). During his experiments, Just observed a physical wave-like lifting of the vitelline envelope around the *Echinarachnius parma* egg, starting from the point of sperm entry, that acted as a physical barrier to sperm entry once fertilization took place. After the initial point of sperm entry, Just saw that sperm near the egg membrane prior to the lifting were immobilized and no longer attempting to enter the egg (Just, 1919). Although it was not yet understood, Just was observing the effects of the fast block to polyspermy through the immobilized sperm and lack of further fertilization near the membrane prior to envelope lifting.

The first electrophysiology recording was made on a frog egg forty years later. Using eggs from the common toad, *Bufo vilagris*, Maéno recorded egg and oocyte membrane potentials in solutions with varying Na^{+}, K^{+}, and Ca^{2+} concentrations in the bath recording solution (Maeno,

1959). Maéno observed no change in membrane potential with increased concentrations of Na^+, K^+, or Ca^{2+} in mature eggs, which was not the case in oocytes, leading to the conclusion that permeability to different ions changes as the oocytes mature into eggs.

These observations and the ability to perform electrophysiology recordings became even more revolutionary in the field when Laurinda Jaffe voltage clamped the membrane of sea urchin egg to establish that the fertilization-signaled depolarization serves as a polyspermy block (L. A. Jaffe, 1976). To do so, she used whole-cell recordings during fertilization of eggs from the purple sea urchin, *Strongylocentrotus purpuratus*. She observed that prior to sperm addition, the resting potential of the eggs was sitting at a negative value (average of -70 mV), and within a few seconds after sperm addition, there was a rapid depolarization of the membrane from the negative resting potential to a less negative fertilization potential (average of -10 mV) (L. A. Jaffe, 1976). These recordings were observed by passively recording the egg's membrane potential.

To then test whether a fertilization-triggered depolarization of the egg membrane could alter the ability of sperm to fertilize, sea urchin eggs were clamped at either the resting potential (-10 mV and lower) or the fertilization potential (over +5 mV) and examined for whether this altered the incidence of fertilization (L. A. Jaffe, 1976). Clamping the eggs at varying membrane potentials was made possible by the invention of the voltage clamp. When eggs were held at a negative potential, multiple sperm fertilized the egg, because this interfered with the fertilization-triggered depolarization and induced polyspermy. Conversely, fertilization was stopped altogether when the eggs were held at the positive potential typically reached after fertilization. Sperm bound to, but did not enter, depolarized eggs (L. A. Jaffe, 1976).

In a well-controlled experiment, the membrane potential was allowed to return to rest, at which time fertilization occurred but not until after the positive hold was released, and the egg

could return to the typical negative resting potential. Interestingly, in addition to not observing fertilization, Jaffe also observed a delay in lifting the fertilization membrane on the egg held at a positive potential compared to the surrounding eggs not clamped at a positive potential (L. A. Jaffe, 1976). The eggs surrounding the positively clamped eggs showed evidence of membrane lifting within the previously observed timeframe from the point of sperm addition. In eggs clamped at a negative potential, although there was no membrane depolarization, the fertilization membrane was lifted, indicating that the slow block to polyspermy still occurred independently of the fast block depolarization (L. A. Jaffe, 1976). Prior to these experiments, the fertilization-signaled depolarization was not known.

Comparative studies on different Amphibians further substantiate that a fertilization-triggered depolarization acts as a polyspermy block. Specifically, it was noted that eggs from polyspermic animals do not depolarize with sperm entry. Moreover, based on the ability of different Amphibians to cross-fertilize, scientists utilized salamanders, frogs, and axolotls to study the effects of membrane current on the sperm's ability to fertilize the egg (Charbonneau, Moreau, Picheral, Vilain, & Guerrier, 1983). This research utilized two species of polyspermic fertilizers (*Pleurodeles* and *Ambystoma*) to compare fertilization events to monospermic species (*Rana temporaria*). It was found that eggs from animals that exhibit polyspermy (*Pleurodeles* or *Ambystoma*) did not depolarize at fertilization and always exhibited polyspermic fertilizations, even when inseminated by sperm from *R. temporaria*, a monospermic species (Charbonneau et al., 1983).

1.2.3.2 Many animals use the fast block to polyspermy

Since the initial recordings of egg membrane depolarizations, the fast block has been observed in a multitude of external fertilizers, including animals from Amphibia (urodele species

clouded salamander *Hynobius nebulosus* (Iwao, 1989) and anurans the American toad *Bufo americanus* (Cross & Elinson, 1980), the northern leopard frog *Rana pipiens* (Cross, 1981; Cross & Elinson, 1980), and the African clawed frog *Xenopus laevis* (Busa, Ferguson, Joseph, Williamson, & Nuccitelli, 1985; Grey, Bastiani, Webb, & Schertel, 1982; L. A. Jaffe, Cross, & Picheral, 1983; Webb & Nuccitelli, 1985)), Echinodermata (sea urchins (L. A. Jaffe, 1976; M. J. Whitaker & Steinhardt, 1983), starfish (Miyazaki & Hirai, 1979; Moccia, Lim, Kyozuka, & Santella, 2004), and sand dollars (Steinhardt, Lundin, & Mazia, 1971)), and even teleost fish (medaka (Nuccitelli, 1980)). Interestingly, although the membrane of medaka eggs depolarizes, this depolarization is not necessary to stop polyspermy, and could be evidence of the analogous evolution of polyspermy blocks in different species as the medaka eggs still depolarize even though the fast block is not required (Nuccitelli, 1980). Notably, of amphibians, the fast block in *X. laevis* is the most complete signaling pathway known out of the species studied (Komondor et al., 2023; Wozniak, Phelps, Tembo, Lee, & Carlson, 2018; Wozniak, Tembo, Phelps, Lee, & Carlson, 2018).

Mammalian eggs, by contrast, do not use the fast block. To explore whether the fast block exists in mammalian eggs, whole-cell recordings were made to determine if fertilization triggered a depolarization of in the membrane or if altering the membrane potential of the eggs could alter the egg's ability to prevent fertilization by multiple sperm. Experiments performed in mice (L. A. Jaffe, Sharp, & Wolf, 1983), rabbits (McCulloh, Rexroad, & Levitan, 1983), and hamsters (Miyazaki & Igusa, 1981, 1982) do not support the existence of a membrane potential reliant polyspermy blocking mechanism.

1.2.3.3 Fast block mechanism

Although it is not yet understood how depolarization of the egg membrane prevents sperm entry, cross-fertilization experiments between gametes from different amphibians suggest that it is likely due to a sperm-derived factor. In a 1983 study, it was demonstrated that the voltage required to prevent sperm from entering the egg was based on the species of sperm rather than the species of egg (L. A. Jaffe, Cross, et al., 1983). For these experiments, *X. laevis* eggs were clamped at varying membrane potentials, and eastern newt (*Notophthalmus viridescens*) sperm was applied. Clamping the eggs at voltages that would keep *X. laevis* sperm out, but not the *Notophthalmus* sperm, did not prevent the fertilization of the egg by the *Notophthalmus* sperm. This experiment was repeated with *Notophthalmus* sperm and *Rana pipiens* (northern leopard frog) eggs, and similar results were seen where the sperm was only kept out when the eggs were clamped at voltages that are typical of a depolarization in *Notophthalmus* eggs (L. A. Jaffe, Cross, et al., 1983). These data indicate that the membrane potential that the egg reaches during the fast block is recognized by sperm of the same species. However, if sperm from a different species is applied, the egg might not depolarize to the correct potential to stop polyspermic fertilization by the different species of sperm. This indicates that the sperm themselves recognize membrane potentials of the egg, and it is not entirely dependent on the egg to keep additional sperm out.

1.3 Details of the fast block in *Xenopus laevis*

1.3.1 Introduction to *X. laevis* as a model

X. laevis serves as a vital model system in fertilization research. These frogs belong to the class Amphibia and order Anura. As external fertilizers, *X. laevis* eggs are abundantly and readily available for laboratory research. The large size of the eggs allows for easier electrophysiology recordings and manipulation during recordings. As opposed to mammalian fertilization, *X. laevis* fertilization is readily accessible in the lab. *X. laevis* produces thousands of eggs in a single experimental day in the lab when induced to ovulate, and these eggs natively use the fast block to polyspermy to keep sperm out of an already fertilized egg. Because *X. laevis* eggs are large, easy to manipulate, and abundant, they have been used as an animal of choice for over 70 years for studying fertilization.

1.3.2 TMEM16A conducts the depolarizing current during the fast block

Prior to the identification of TMEM16A as the ion channel involved in the fast block to polyspermy, experimental evidence suggested that a Ca^{2+}-mediated Cl^- efflux depolarized the eggs from *X. laevis*. In these experiments, fertilization recordings of *X. laevis* eggs were conducted in solutions of varying Cl^- concentrations. Reducing extracellular Cl^- yielded larger depolarizations as expected for a Cl^- conducted current because of the increased driving force behind the Cl^- movement out of the egg. The inverse of this was also true, whereby increasing extracellular Cl^- led to smaller depolarizations (Grey et al., 1982; Webb & Nuccitelli, 1985). Scientists took advantage of the ability of Cl^- channels to conduct other halides (Wright & Diamond, 1977). When

recording from *X. laevis* eggs in solutions where Cl^- was replaced with other halides, such as I^- and Br^-, fertilization did not change the membrane potential when eggs were inseminated in Br^-, whereas fertilization triggered a hyperpolarization when eggs were fertilized in I^- -enriched solutions (Grey et al., 1982; Watabe et al., 2019). These conditions also led to polyspermic fertilization (Grey et al., 1982; Watabe et al., 2019). These data demonstrate that fertilization opens a Cl^- channel in *X. laevis* eggs during the fast block to polyspermy.

Previous research in the Carlson Lab identified TMEM16A as the Cl^- channel responsible for the fast block to polyspermy in *X. laevis* (Wozniak, Phelps, et al., 2018). To do so, published proteomics and RNA-sequencing datasets were interrogated to uncover two candidate Cl^- channels that localize to the plasma membrane and could potentially conduct the depolarizing Cl^- current: TMEM16A and BEST2A. Notably, both TMEM16A and BEST2A are Ca^{2+}-activated Cl^- channels. TMEM16E and TMEM16K were also identified in this screen as both have been annotated as Cl^- channels; however, both function as ER-localized lipid scramblases and, therefore, were ruled out as having a role in depolarizing *X. laevis* eggs during the fast block (Wozniak, Phelps, et al., 2018). Both TMEM16A and BEST2A channels are present in fertilization-competent *X. laevis* eggs.

Following the identification of two candidate Cl^- channels, Wozniak and colleagues exogenously expressed BEST2A in axolotl (*Ambystoma mexicanum*) oocytes and performed two-electrode voltage clamp electrophysiology recordings. Axolotl oocytes were chosen because these cells lack other Ca^{2+}-activated currents (Schroeder, Cheng, Jan, & Jan, 2008). Using a photolabile caged-IP_3, axolotl oocytes expressing either TMEM16A or BEST2A exhibited large currents with light application, substantiating that both channels act as Ca^{2+} activated Cl^- channels. Another

research group has previously showed similar results for exogenous expression of TMEM16A in axolotl oocytes (Schroeder et al., 2008).

Using the axolotl oocytes expressing either TMEM16A or BEST2A, various inhibitors were screened with the goal of identifying compounds capable of discriminating currents conducted by the two channels to determine then which channel is used during the fast block. Of the five inhibitors screened, Ani9 and MONNA significantly inhibited TMEM16A-conducted currents while nominally acting on BEST2A channels (Wozniak, Phelps, et al., 2018). When Ani9 and MONNA were used during whole-cell recordings during fertilization of *X. laevis* eggs, there was a significant slowing or complete lack of depolarization in each inhibitor, respectively, and polyspermic development occurred. These findings demonstrate that fertilization signals the Ca^{2+}-activated Cl^- channel TMEM16A opening, which conducts an efflux of Cl^- to depolarize *X. laevis* eggs during the fast block to polyspermy (Wozniak, Phelps, et al., 2018).

1.3.3 The fast block is mediated by the production of IP_3 from PLC activation

Additional research in the Carlson Lab examined the source of Ca^{2+} that activates TMEM16A. First, Wozniak et al. examined whether *X. laevis* eggs need Ca^{2+} to initiate the fast block. Using Ca^{2+} channel inhibitors, they examined that the fast block depolarization and polyspermy rates remained unchanged compared to control conditions. This study established that IP_3 is necessary for the membrane depolarization as the fast block did not occur when using IP_3 receptor inhibitors during whole-cell recordings (Wozniak, Tembo, et al., 2018) In addition to needing functional IP_3 receptors, phospholipase C (PLC) is also required for the fast block, as inhibiting it prevents the fast block and led to polyspermy (Komondor et al., 2023; Wozniak, Tembo, et al., 2018). This research showed that the elevated Ca^{2+} that is responsible for activating

TMEM16A in *X. laevis* eggs, which has been confirmed by multiple research groups, including the Carlson lab (Grey et al., 1982; Kline, 1988; Nuccitelli, Yim, & Smart, 1993; Wagner, Li, Pearson, & Keizer, 1998; Watabe et al., 2019; Wozniak, Phelps, et al., 2018; Wozniak, Tembo, et al., 2018), comes from a PLC/IP_3-mediated cytoplasmic Ca^{2+} increase. Early experiments examined the speed and concentration of Ca^{2+} released at fertilization in *X. laevis* eggs and showed that the Ca^{2+} is rapidly released in a wave around the egg from the point of sperm entry at a rate as quick as 17.2 μM/s with a concentration as high as 1.2 μM (Fontanilla & Nuccitelli, 1998).

During the fast block to polyspermy in *X. laevis*, fertilization triggers the activation of PLC, which cleaves PIP_2 into its two secondary messengers, DAG and IP_3. Currently, there is no evidence that DAG plays a role in the fast block to polyspermy. However, IP_3 binds to the IP_3 receptor in the ER, initiating an increase in cytoplasmic Ca^{2+} that activates TMEM16A in the egg membrane. TMEM16A activation causes an efflux of Cl^- that depolarizes the egg membrane to prevent further sperm entry (Figure 1). Although it is well established that PLC is needed, it remains unclear how fertilization causes the activation of PLC during the fast block to polyspermy.

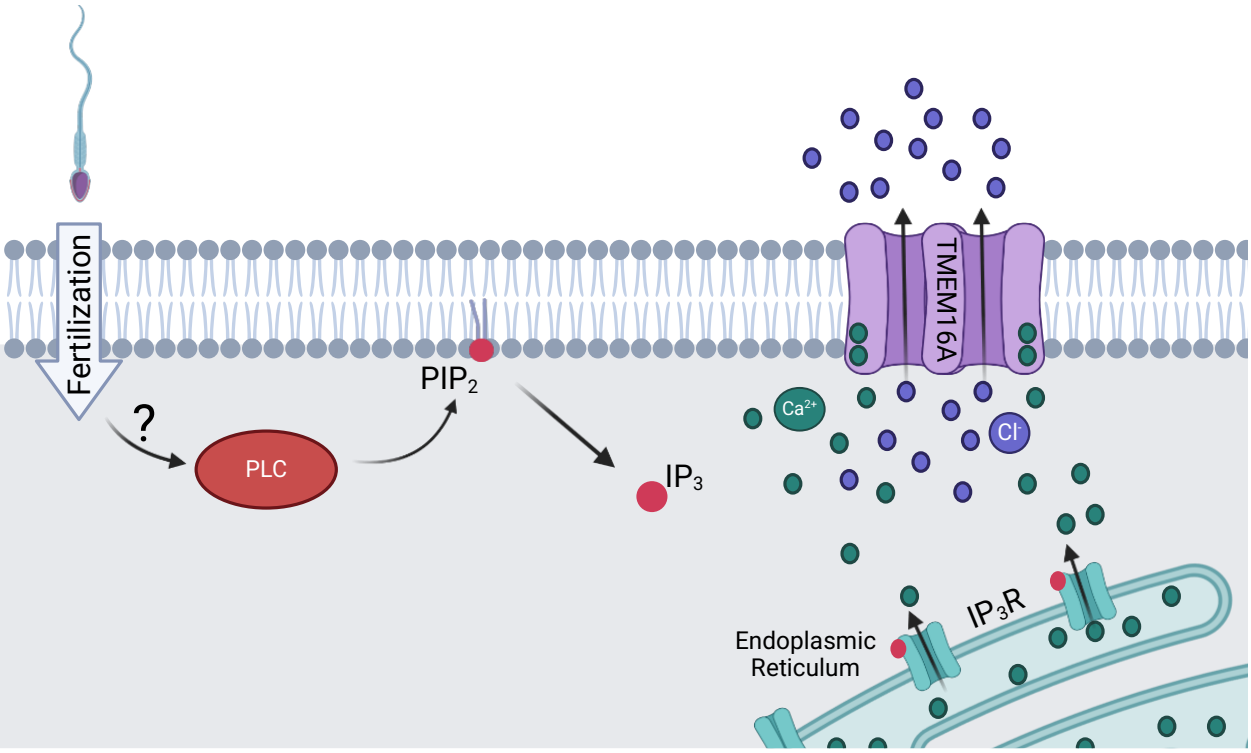

Figure 1: The fast block to polyspermy pathway in *X. laevis*.

Fertilization activates phospholipase C (PLC) through an unknown mechanism. PLC cleaves phosphatidylinositol 4,5-bisphosphate (PIP_2) to create the second messenger inositol trisphosphate (IP_3). IP_3 binds to the IP_3 receptor in the endoplasmic reticulum (ER) to release Ca^{2+} from intracellular stores. Ca^{2+} activates TransMEMbrane 16A (TMEM16A), which releases Cl^- to depolarize the membrane and prevent further sperm entries in the egg.

1.4 Phospholipase C

1.4.1 Background of PLCs

Phospholipase Cs (PLCs) comprise a group of membrane-associated enzymes that cleave the acidic phospholipid phosphatidylinositol-4,5-bisphosphate (PIP_2) into two secondary messengers, diacylglycerol (DAG) and inositol 1,4,5-trisphosphate (IP_3) (Bill & Vines, 2020; Gresset, Sondek, & Harden, 2012). While these secondary messengers are important for a multitude of cellular processes, including polyspermy prevention, it is interesting that there are many different PLC subtypes that are responsible for creating these same products.

PLCs are classified based on their method of activation and structural conservation. There are 6 recognized PLC subtypes, and there are multiple isozymes within these groups. All PLC subtypes share the same basic architecture, regardless of the activation method, except PLCζ, which is slightly different structurally. These 4 conserved enzyme components include a pleckstrin homology (PH) domain, four consecutive EF hands, the triosephosphate isomerase (TIM) barrel composed of nearly identical X and Y domains, and a C2 domain (Figure 2) (Bill & Vines, 2020; Gresset et al., 2012; Kawakami, Xiao, Yasudo, & Kawakami, 2012).

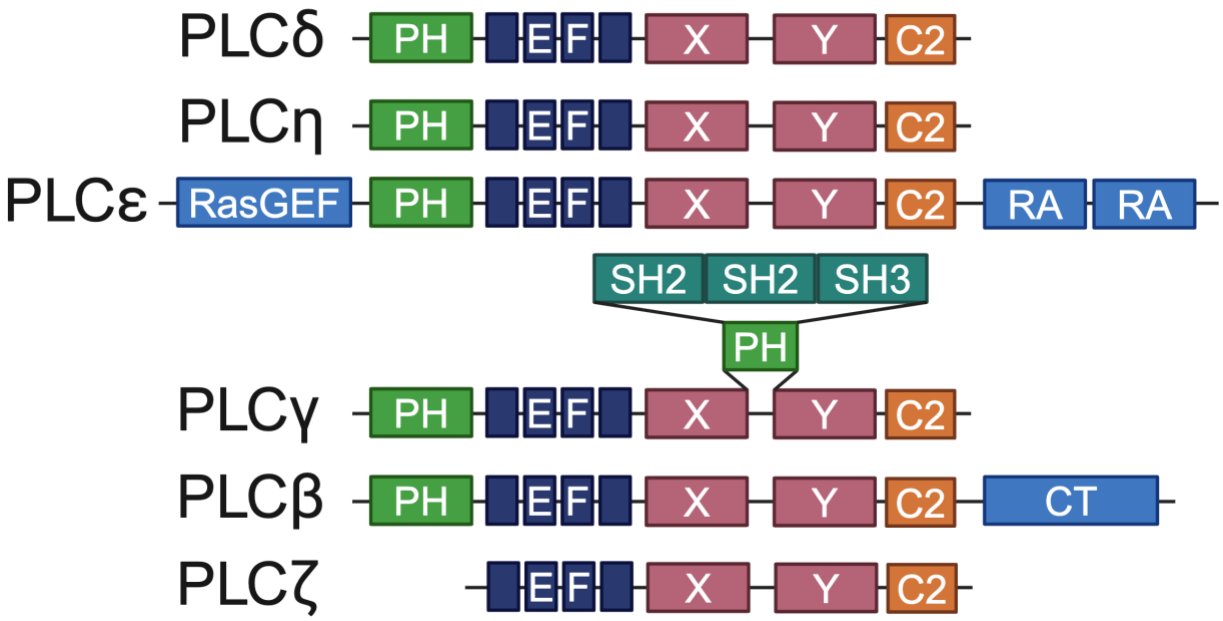

Figure 2: PLC structures organized by isozyme.

PH: Pleckstrin homology domain. EF: EF Hands. X-Y: TIM barrel, separated into X-Y domains. RasGEF: Ras guanine exchange factor. RA: Ras-associated domains. SH: Src homology domains. CT: C-terminal domain.

The PH domain is responsible for tethering the PLCs to the membrane phospholipids, such as PIP_2. Notably, PLCζ is a soluble PLC, as it is the only isoform that does not contain a PH domain. The EF hands bind Ca^{2+} and has different functions depending on the PLC isozyme, and although Ca^{2+} binds to this domain in some PLC isozymes, it is not thought to be a regulatory binding process (Kawasaki & Kretsinger, 1994). The active site of PLC is located in the TIM barrel, along with the catalytic residues and a Ca^{2+} binding site, and is divided into two sections, X and Y domains. Within the TIM barrel is also an autoinhibitory section called the X-Y linker that is removed when PLC is activated, as it occludes the active site when the enzyme is not activated (Gresset et al., 2012). The C2 domain of the enzyme is important for signal transduction and membrane interaction (Bill & Vines, 2020). The conservation of various Ca^{2+} binding sites is interesting, as all PLC subtypes, while each having its own methods of activation, can also be

activated by Ca^{2+} with varying affinity and activity levels (Rhee, 2001). While there are these conserved domains within the PLC subtypes, there are also additional domains in some PLCs, and the functions of these domains differ in different subtypes. These different functions also relate to how the PLCs are activated and comprise the differences between the PLC isoforms.

1.4.2 PLCδ and PLCη

PLCδ and PLCη are composed of only the four essential structural domains. PLCδ isozymes are typically activated via membrane association with PIP_2 binding near the PH domain and Ca^{2+} binding near the C2 domain. Notably, PLCδ is the only PLC subtype that is activated most sensitively by Ca^{2+}, although Ca^{2+} activates all PLCs with some affinity (Gresset et al., 2012). PLCδ can also hydrolyze multiple PIP_2 molecules in a single binding event at the plasma membrane within the PH domain (Lomasney et al., 1996), as this domain interacts with the membrane phospholipids such as PIP_2.

Once activated, PLCδ1 moves between the nucleus and the cytoplasm, whereas, in quiescent cells, it remains in the cytoplasm. When this isozyme is depleted, there is an arrest in the cell cycle (Stallings, Tall, Pentyala, & Rebecchi, 2005). δ1 also plays a role in skin homeostasis, hair growth and loss, tumor promotion, Alzheimer's disease, and hypertension (Bill & Vines, 2020). PLCδ3 is responsible for the regulation of microvilli formation in the intestines and directing neuron migration within the cerebral cortex during brain development (Kouchi et al., 2011; Sakurai, Hirata, Yamaguchi, Nakamura, & Fukami, 2011). PLCδ4 localizes mostly to the nucleus of mesenchymal stem cell-derived adipose tissue cells (Kunrath-Lima et al., 2018).

Interestingly, PLCδ4 knockout mice are sterile, likely due to the dysregulation of Ca^{2+} required for the acrosome reaction (Fukami et al., 2001; Fukami et al., 2003).

While PLCη is structurally similar to PLCδ, less is known about its activation mechanisms, although there is evidence that PLCη is activated by Gβγ and is, therefore, downstream of the GPCRs (Zhou, Sondek, & Harden, 2008; Zhou, Wing, Sondek, & Harden, 2005). PLCη has been implicated in infant brain development (Nakahara et al., 2005), and a loss of PLCη has been linked to Alzheimer's disease (Popovics & Stewart, 2012) and mental delays (Lo Vasco, 2011), indicating that PLCη is essential for proper brain development and function.

1.4.3 PLCε

PLCε has three unique domains: Ras guanine-exchange factor (RasGEF) and two tandem Ras-associated (RA) domains. While PLCs are important for phospholipid signaling pathways involving PIP_2 and its two products, the additional domains of PLCε are important for the integration of other signaling pathways that involve heterotrimeric and Ras family G proteins. This means that this PLC is also capable of exchanging GTP for GDP of Ras family small GTPases (Boguski & McCormick, 1993). PLCε is activated via a GPCR-mediated pathway, as it is activated by the Gβγ subunit directly, and a number of other heterotrimeric G protein subunits indirectly (Bill & Vines, 2020; Wing et al., 2001). Notably, it is also activated by $G\alpha_{12/13}$ indirectly, as $G\alpha_{12/13}$ activate Rho, which directly binds to PLCε to activate (Wing, Bourdon, & Harden, 2003; Wing, Snyder, Sondek, & Harden, 2003).

PLCε is most highly expressed in the heart, liver, and lungs, but is also found in other tissues, including the testis, uterus, and skeletal muscles (Bill & Vines, 2020). It has been

suggested to be important for inflammation response, heart development, and cancer development and progression (Bill & Vines, 2020).

1.4.4 PLCγ

PLCγ has an additional PH domain, aside from the N-terminally located PH domain, in the X-Y linker of the TIM barrel that contains two Src homology 2 (SH2) and one Src homology 3 (SH3) domains (Gresset et al., 2012). PLCγ is activated via tyrosine phosphorylation of the SH2 domains, and these pathways are activated by either receptor or non-receptor tyrosine kinases (Gresset, Hicks, Harden, & Sondek, 2010). This phosphorylation causes a conformational change that removes the autoinhibitory aspect of the PLC in the X-Y linker region of the TIM barrel (Gresset et al., 2010). In addition to phosphorylation, there is evidence that PIP_3 interacts with the PH domain (Falasca et al., 1998) and the SH2 domain (Bae et al., 1998) in PLCγ1 and gives rise to docking sites to the plasma membrane of cells. However, the mechanisms behind the increased activity from this activation method remain an area of active research. For example, additional research suggests that PLCγ1 can be activated by phosphatidic acid, a byproduct from the cleavage of phosphatidylcholine by phospholipase D (Jones & Carpenter, 1993).

PLCγ1 is ubiquitously expressed, whereas PLCγ2 is mostly expressed in hematopoietic cells downstream of immune cell receptors. PLCγ has been reported to play a role in signaling in B and T cells, calcium fluxes, tumor formation, and cell differentiation and proliferation (Bill & Vines, 2020).

1.4.5 PLCβ

In addition to the four previously mentioned conserved domains shared with other PLCs, PLCβ has a C-terminal coiled-coil domain that is thought to play a role in dimerization, membrane association, and activation via the Gα subunits of heterotrimeric G-protein coupled receptors in certain PLCβ subtypes (Ilkaeva, Kinch, Paulssen, & Ross, 2002; Singer, Waldo, Harden, & Sondek, 2002). In addition to activation via specific Gα subunits, namely $G\alpha_q$, $G\alpha_{11}$, $G\alpha_{14}$, and $G\alpha_{15}$, PLCβ is also activated by Gβγ (Boyer, Waldo, & Harden, 1992; Camps et al., 1992). Gβγ activates PLCβ through direct binding, although the binding interface is not exactly known but is suggested to be in the C-terminal domain (CTD), which causes a release of the autoinhibitory interaction caused by the CTD (Fisher, Jenkins, Tall, Burke, & Smrcka, 2020).

PLCβ play numerous roles in cellular regulation and disease progression and is expressed in many tissues throughout the body. PLCβ1 often localizes in the nucleus of the cell and is thought to regulate the cell cycle. It is highly expressed in the cerebral cortex, hippocampus, cardiomyocytes, and retina (Bill & Vines, 2020). PLCβ4 is also expressed throughout the brain. Mis-regulation of β1 and β4 have been connected to numerous brain conditions including Alzheimer's, Huntington's, and bipolar disease, and depression (Bill & Vines, 2020).

PLCβ2 is expressed in hematopoietic cells and has been suggested to play a role in different cancers. Interestingly, increasing PLCβ2 expression has been suggested as a potential therapy for triple negative breast cancer (Brugnoli et al., 2017). Although less is known about the role of PLCβ3, it has been shown to be expressed in the liver, brain, and parotid gland, and is thought to contribute to neutrophil development (Kawakami & Xiao, 2013).

1.4.6 PLCζ

PLCζ is a sperm-specific PLC that is expressed in the sperm of mammals and some frogs and is the smallest PLC, as it lacks the PH domain, making it the only PLC that is not membrane-bound (Saunders et al., 2002). PLCζ has the highest sensitivity to activation via Ca^{2+} out of all PLC isozymes (Kouchi et al., 2004). In mammalian fertilization, PLCζ is needed to increase intracellular Ca^{2+} concentrations to prevent multi-sperm fertilizations. Upon sperm-egg fusion in mammals, the soluble PLCζ enters the egg and causes an increase in cytoplasmic Ca^{2+} via the cleavage of PIP_2 to create IP_3 that releases internal Ca^{2+} stores from the ER. PLCζ is encoded by the PLCZ1. This gene is conserved in mammals and most amphibians but is missing in the genomes of all pipoid frogs including *X. laevis* (Bainbridge, Rosenbaum, Sau, & Carlson, 2023).

1.5 Summary of research goals

With over 100 years of research providing details and evidence of an immediate polyspermy-blocking mechanism, some of the details of this pathway remain unknown. In *X. laevis*, native users of the fast block, it has been established that TMEM16A opens via a PLC-mediated cytoplasmic Ca^{2+} increase that causes the egg membrane to depolarize to prevent further sperm entry following fertilization (Wozniak, Phelps, et al., 2018; Wozniak, Tembo, et al., 2018). My dissertation research sought to identify the still elusive activation mechanism of phospholipase C during the fast block to polyspermy in *X. laevis*. Part of this work has been published in a manuscript in the Journal of General Physiology (Komondor et al., 2023).

2.0 Methods

2.1 Reagents

Genistein was obtained from Alfa Aesar (Thermo Fisher Scientific; Tewksbury, MA), Lavendustin A/B were purchased from Santa Cruz Biotechnology (Dallas, TX), and human chorionic gonadotropin was purchased from Covetrus (Dublin, OH). Leibovitz's-15 (L-15) medium (without L-glutamine) was obtained from Sigma-Aldrich. YM-254890 was purchased from Tocris Bio-Techne Corporation (Minneapolis, MN). U73122 was obtained from Cayman Chemical (Ann Arbor, MI). All other materials, unless noted, were purchased from Thermo Fisher Scientific.

2.2 Solutions

Modified Ringers (MR) solution (100 mM NaCl, 1.8 mM KCl, 2.0 mM $CaCl_2$, 1.0 mM $MgCl_2$, 5.0 mM HEPES, pH 7.8) was filtered using a sterile, 0.2 μM polystyrene filter and was used as the base for all fertilization and electrophysiology recordings in this dissertation. The MR solution was diluted for whole-cell recordings during fertilization (20% - MR/5) with or without indicated inhibitors and for embryo incubation following fertilization recordings (33% - MR/3). Concentrated stock solutions made in DMSO were diluted for MR solutions supplemented with inhibitors. Final DMSO content was maintained below 2% solution, a concentration that does not alter with the fast block (Wozniak, Tembo, et al., 2018).

The solutions OR2 (82.5 mM NaCl, 2.5 mM KCl, 1 mM $MgCl_2$, 5 mM HEPES, pH 7.6) and ND96 (96 mM NaCl, 2 mM KCl, 1.8 mM $CaCl_2$, 1 mM $MgCl_2$, 5 mM HEPES, 5 mM sodium pyruvate, gentamycin, pH 7.6) were used for collection and storage of immature oocytes. Before use, these solutions were filtered using a sterile, 0.2 μM polystyrene filter.

2.3 Animals

All animal procedures were conducted using acceptable standards of humane animal care and approved by the Animal Care and Use Committee at the University of Pittsburgh. *X. laevis* adults obtained commercially from the University of Chicago Marine Biological Laboratory (Woods Hole, MA), Nasco (Fort Atkinson, WI), or Xenopus 1 (Dexter, MI). They were housed at 20°C with a 12-h/12-h light/dark cycle.

2.4 Collection of gametes

2.4.1 Fertilization-competent eggs

Sexually mature *X. laevis* females were injected with 1,000 IU human chorionic gonadotropin into the dorsal lymph sac and housed overnight at 16 °C for 12-16 hours to induce ovulation (Wozniak et al., 2017). Females typically began laying within 2 hours of being moved to room temperature. Eggs were collected on dry Petri dishes and used within 10 min of laying.

2.4.2 Sperm

Testes were harvested from sexually mature *X. laevis* males to obtain sperm for fertilization experiments (Wozniak et al., 2017). Males were euthanized by a 30-minute immersion in 3.6 g/L MS-222, pH 7.4, before testes were harvested and cleaned. Testes were then stored at 4 °C in L15 Leibovitz's Medium without glutamine for use up to 1 week later.

2.4.3 Oocytes

X. laevis oocytes were collected by obtaining ovarian sacs from mature *X. laevis* females anesthetized with a 30-minute immersion in 1.0 g/L MS-222, pH 7.4. Ovarian sacs were manually pulled apart with forceps and incubated for 90 min in 1 mg/mL collagenase dissolved in ND96. Collagenase was removed by repeated washes with OR2, followed by washes in ND96, and healthy oocytes were sorted before storage at 12 °C in ND96.

2.5 Electrophysiology

Electrophysiological recordings were made using TEV-200A amplifiers (Dagan Co.) and the Axon Digidata 1550A digitizer (Molecular Devices). Data were acquired with pClamp Software (Molecular Devices) at a rate of 5 kHz. Borosilicate glass pipettes used to impale the *X. laevis* eggs for recordings were made with a Model P-87 Flaming/Brown Micropipette puller (Sutter Instruments) for a resistance of 0.5-15 MΩ. Pipettes were filled with 1 M KCl.

2.5.1 Whole-cell recordings

The membrane potentials of eggs before (resting potential) and after fertilization (fertilization potentials) were quantified approximately 10 s before and after the depolarization. Depolarization rates of each recording were quantified by determining the maximum velocity of the quickest 1-mV shift in the membrane potential (Wozniak, Phelps, et al., 2018).

2.5.2 Two-electrode voltage clamp (TEVC) recordings

The efficacy of inhibitors targeting PLCβ activation was screened by recording native TMEM16A currents in the two-electrode voltage clamp configuration on *X. laevis* oocytes clamped at -80 mV. Blue/green light was applied using a 250 ms exposure to light directed from the opE-300^{white} LED Illumination System (CoolLED Ltd) and guided by a liquid light source to the top of the oocytes expressing the light-activated muscarinic receptor, opto-M1R (Morri et al., 2018), in 35 mm Petri dishes. Background-subtracted peak currents were quantified and compared between two consecutive recordings. In control recordings, measurements were taken 10 min apart, and in inhibitor screens, one recording was taken before and one during the application of screened inhibitors after a 10-min incubation. The proportional difference between peak currents before and with the inhibitor for each oocyte was used to quantify inhibition.

2.6 Polyspermy Assay

Inseminated eggs used during whole-cell recordings were kept for observation for 2 hours to determine the incidence of polyspermy with or without inhibitors. Symmetrical cleavage patterns defined successful monospermic fertilization furrows at 90 and 120 mins in embryos, while polyspermic fertilization was defined by asymmetric patterns of cleavage furrows (Elinson, 1975; Grey et al., 1982).

2.7 Bioinformatics

To identify the PLC isoforms present in mature *X. laevis* eggs, existing transcriptomic (Session et al., 2016) and proteomic (Wuhr et al., 2014) datasets were quarried for "PLC" genes. RNA sequencing data was obtained from *X. laevis* oocytes at different stages of development as well as from the fertilization-competent eggs (Session et al., 2016). The proteomic dataset obtained from mature de-jellied *X. laevis* whole egg lysates was analyzed using liquid chromatography-mass spectrometry (Wuhr et al., 2014).

2.8 Exogenous protein expression in *X. laevis* oocytes

The cDNAs encoding the platelet-derived growth factor receptor (PDGF-R) (Gagoski et al., 2016) or the rhodopsin-muscarinic receptor type 1 chimera (opto-M1R) (Morri et al., 2018) were purchased from Addgene (plasmids 67130 and 106069 respectively) and engineered into the

GEMHE vector using overlapping extension PCR. The sequences for all constructs were verified by automated sequencing (Gene Wiz or Plasmidsaurus) and were transcribed to cRNA using the T7 mMessage mMachine (Ambion). Defolliculated oocytes were injected with cRNA and used in experiments 2-3 days after injection to allow expression.

2.9 Removal of egg jelly

For procedures requiring the removal of jelly, eggs were incubated at room temperature either in inhibitor treatments or control conditions before insemination with sperm suspension prepared as described previously (Wozniak et al., 2020). Eggs used in the inhibitor screen were incubated in inhibitors for 10 min before insemination. Activated eggs, an indicator of successful fertilization, were identified by their ability to roll so the animal pole faced up and displayed a contracted animal pole. To remove the jelly layer, activated eggs for western blots were placed on 2% agar in MR/3 in a 35 mm petri dish in MR/3 with 45 mM β-mercaptoethanol (BME), pH 8.5. During the BME incubation, eggs were gently agitated for 1-2 min until their external jelly visibly dissolved. To remove the BME solution, de-jellied eggs were moved with a plastic transfer pipette with as little BME solution as possible to a 2% agar in MR/3-coated Petri dish in MR/3 pH 6.5 and agitated for an additional minute. Eggs were then transferred three more times to additional agar-coated dishes with MR/3 pH 7.8, swirling gently and briefly in each.

2.10 Sample preparation and western blot

Oocytes and de-jellied eggs were lysed using a Dounce homogenizer and ice-cold oocyte homogenization buffer (OHB) (10 mM HEPES, 250 mM sucrose, 5 mM $MgCl_2$, 5% glycerol supplemented with protease and phosphatase inhibitors in a 1:100 dilution) (Hill et al., 2005). 10 μL of OHB was used per one egg or oocyte, for a total of 100 μL with 10 eggs or oocytes in each western blot sample preparation. Cellular debris and yolk were removed by centrifugation at 500 RCF for 5 mins at 4 °C. The supernatant was transferred to a new tube, and the resulting pellet was then resuspended in 100 μL OHB. The sample was again sedimented, and the supernatant from both sedimentations was pooled and centrifuged at 18,213 RCF for 15 mins at 4 °C. The supernatant was transferred to a new tube and then sedimented again at 18,213 RCF for 15 mins at 4 °C. 30 μL of this supernatant was combined with 10 μL sample loading buffer (50 mM Tris pH 6.8, 2% SDS, 10% glycerol, 1% β-mercaptoethanol, 12.5 mM EDTA, 0.02% bromophenol blue) before incubating at 95 °C for 1 min.

Egg and oocyte lysates were resolved by electrophoresis on precast 4-12% BIS-TRIS PAGE gels (Invitrogen) run in TRIS-MOPS (50 mM MOPS, 50 mM Tris, 1 mM EDTA, 0.1% SDS) buffer, followed by wet transfer to a nitrocellulose membrane at 10 V for 1 hour in Bolt (Invitrogen) transfer buffer. Protein loading was evaluated by Ponceau staining. Blocking on nitrocellulose was performed for 1 hour at room temperature using Superblock (Thermo) buffer. Primary antibody incubation was performed overnight at 4 °C with anti-phosphorylated PLCγ[pY783] (Abcam) (1:1000), and secondary antibody was performed for 1 hour at room temperature using goat anti-rabbit HRP (Invitrogen) (1:10000). All washes were performed using

TBST (20 mM Tris, 150 mM NaCl, 0.1% Tween-20, pH 8). Using chemiluminescence settings, the blots were imaged using Supersignal Pico (Pierce) on a GE/Amersham 600RGB image.

2.11 Quantification and statistical analyses

All electrophysiology recordings were analyzed and edited with Igor (WaveMetrics), Prism (GraphPad), Excel (Microsoft), and Illustrator (Adobe). Data for each experimental condition are displayed in Tukey box plot distributions, where the box contains the data between 25% and 75%, and the whiskers span 10-90%. All control and experimental conditions include trials conducted on multiple days using gametes from multiple individuals, and depolarization rates were $\log_{10}$ transformed before statistical analyses. Analysis of variance (ANOVA) with post hoc Tukey honestly significant difference test was used to determine differences between control and inhibitor treatments. Figure schematics were created in BioRender.

3.0 Results

3.1 Fertilization signals a depolarization in *X. laevis* eggs

To study the fast block to polyspermy, I made whole-cell recordings on *X. laevis* eggs during fertilization. To do so, I placed a freshly laid *X. laevis* egg in a Petri dish containing approximately 3 mL of MR/5 (Figure 2A). After determining the resistance of the borosilicate pipette tips (between 0.3-21.7 MΩ), I used these tips to impale the egg. Prior to fertilization, I observed an average resting potential for eggs in control conditions of -13.4 ± 1.0 mV (Figure 2B, N=44). After obtaining a steady resting potential, I applied minced testis to the egg. Typically, I observed a fertilization-signaled depolarization of 6 ± 0.5 min following sperm application (N=44). The depolarization is marked by a rapid increase in the membrane potential, as shown in Figure 2C. I quantified the depolarization rate is the fastest 1 mV shift, as this rate is directly proportional to the number of channels opened that allow for the membrane to depolarize. The mean rate of depolarization was 6.7 ± 1.9 mV/ms (Figure 2D). This depolarized membrane potential observed following the fertilization, or the fertilization potential, was 3.2 ± 1.8 mV (N=44, Figure 2B).

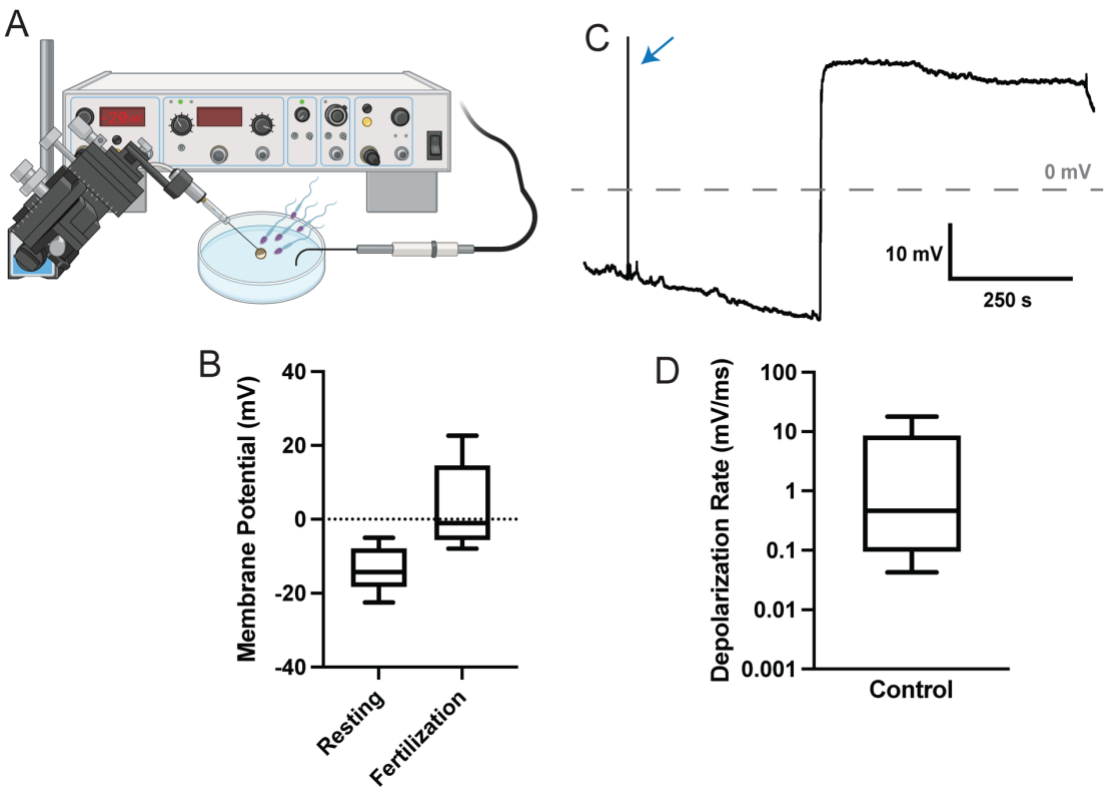

Figure 3: Fertilization evokes a depolarization in *X. laevis*.

(A)Whole-cell recording set up. *X. laevis* egg is impaled with an electrode that passively records the membrane potential of the egg during fertilization recordings. (B) Tukey box plot distributions of the resting and fertilization membrane potentials in control conditions (N=44). (C) Representative whole-cell recording made in control conditions, with MR/5 solution. The blue arrow indicates the time of sperm addition. The gray dashed line denotes zero mV. (D) Tukey box plot distribution of the depolarization rate in control conditions (N=44). The box plot middle lines denotes the median values, the boxes indicate 25-75%, and the whiskers represent 10-90% of the data distributions.

3.2 PLC is required to signal a depolarization in *X. laevis* eggs during fertilization

During fertilization, Ca^{2+} opens the Ca^{2+}-activated Cl^- channel TMEM16A, which then conducts a depolarizing efflux of Cl^- that depolarizes the membrane. The Ca^{2+} that activates the channel is released from the endoplasmic reticulum following the fertilization-signaled activation of PLC (Wozniak, Tembo, et al., 2018). Similar to previous research from our lab, I have found that inhibiting PLC completely stopped the fast block in *X. laevis* (Figure 3A) (Wozniak, Phelps, et al., 2018). In nine independent recordings, fertilization did not evoke a depolarization in *X. laevis* eggs in the presence of 1 μM U73122 (Figure 3B), and the resting potential was similar to what was seen in control conditions (-13.4 ± 1.0 mV in control conditions versus -12.5 ± 1.0 mV in U73122, P= 1.0, Figure 3C), and all 9 eggs developed asymmetric cleavage furrows, consistent with polyspermic fertilization (Figure 3D) (Elinson, 1975; Grey et al., 1982). These results substantiate a requirement for PLC to activate the fast block in *X. laevis* eggs.

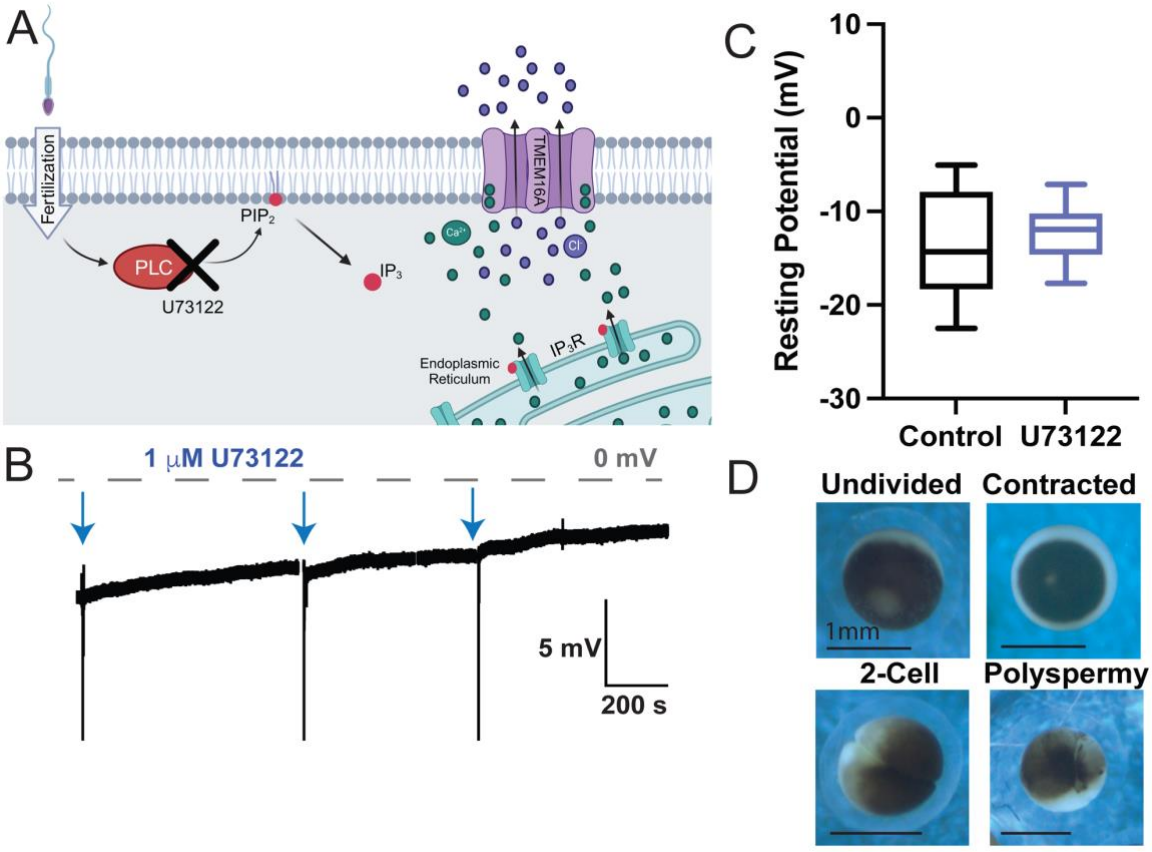

Figure 4: U73122 inhibits PLCs during the fast block to polyspermy in *X. laevis*.

(A) U73122 inhibits PLC during the fast block to polyspermy. (B) Shown is a representative whole-cell recording that was made in the presence of 1 μM U73122. The gray dashed line denotes zero mV. The blue arrows denote three separate sperm additions. (C) Tukey box plot distributions of the resting membrane potential in control conditions (*black*, N=44) and 1 μM U73122 (*blue*, N=9). The middle line denotes the median value, the box indicates 25-75%, and the whiskers represent 10-90% of the data distribution. (D) Representative images of undivided, activated and contracted, monospermic 2-cell divided, and polyspermic *X. laevis* eggs.

3.3 An egg-derived PLC is responsible for evoking the fast block in *X. laevis*

I sought to uncover the origin of the PLC necessary to initiate the fast block. At fertilization, two different cells – sperm and egg – fuse to form the nascent zygote. Theoretically, the PLC that signals the fast block could be provided by either gamete. I interrogated whether the PLC necessary for the fast block is egg or sperm derived in *X. laevis* fertilization. Notably, the functional moiety on U73122 is a maleimide and is therefore predicted to inhibit PLC using a covalent modification of cysteines in the active site of the enzyme (Bleasdale et al., 1989). This covalent modification should yield an irreversible inhibition. Thus, I sought to identify which gamete provides the PLC that signals the fast block by inhibiting the PLCs in each gamete before fertilization. To do so, I separately pretreated sperm and eggs with 1 μM U73122, mixed the gametes in the absence of the inhibitor, and assayed for the fast block using whole-cell recordings (Figure 4A). I found that fertilization evoked normal depolarizations when *X. laevis* sperm were pretreated with 1 μM U73122 for 10 mins prior to application on the egg during whole-cell recordings (Figure 4B). For these recordings, eggs had a typical resting (-15.1 ± 4.1 mV, N=5, *P*=1.0 Figure 4C) and fertilization (3.8 ± 1.8, N=5, *P*=1.0 Figure 4C) potentials that were not significantly different from control conditions (vs -13.4 ± 1.0 mV and 3.2 ± 1.8 mV for controls, respectively). Similarly, in sperm pretreatment experiments, the rate of depolarization (10.6 ± 8.6 mV/ms, N=5 Figure 4D) was not significantly different from control (6.7 ± 1.9 mV/ms, *P*=0.99) conditions. This result suggests that a sperm-derived PLC does not signal the fast block in *X. laevis* fertilization.

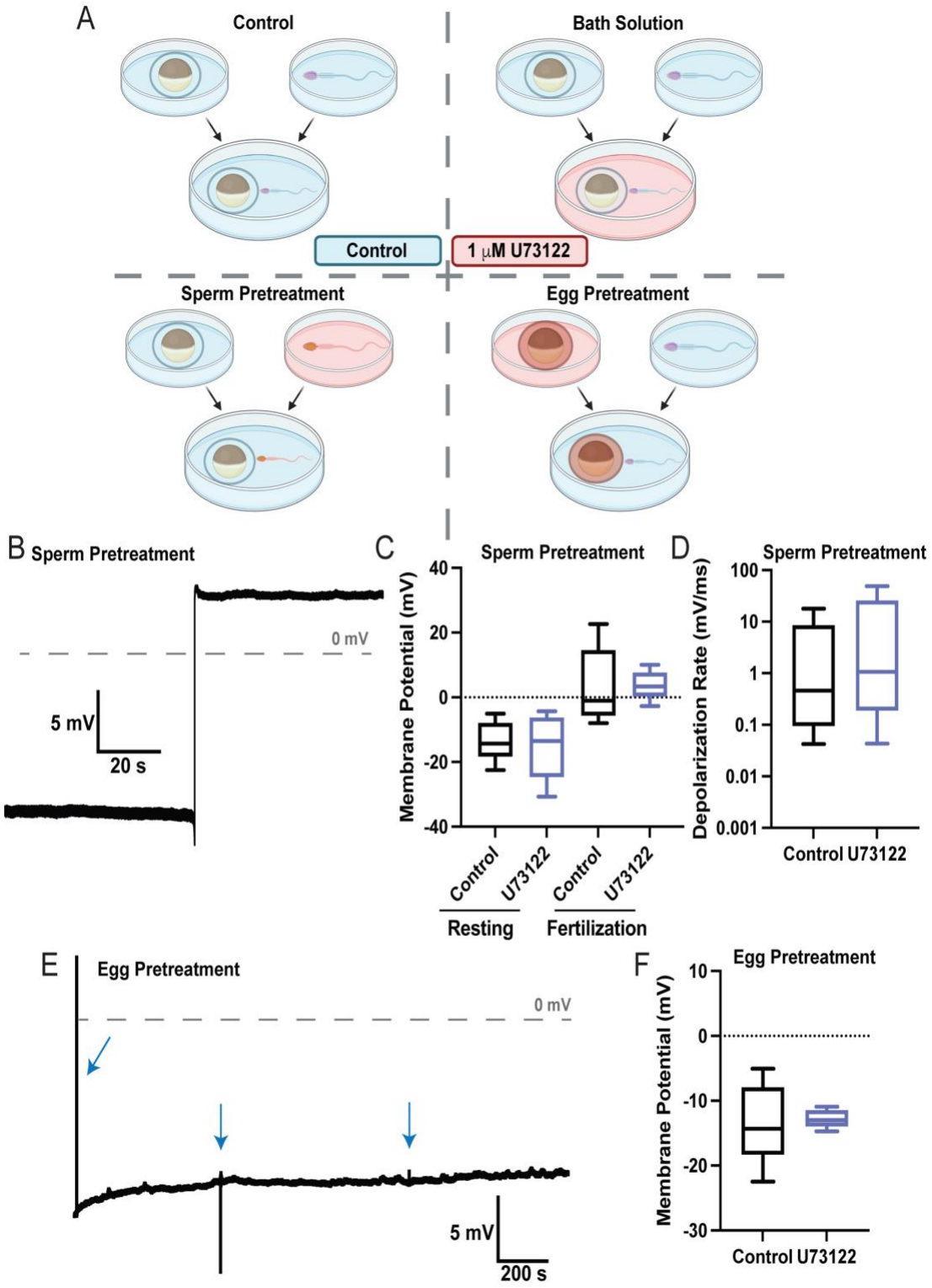

Figure 5: An egg-derived PLC is activated during the fast block to polyspermy in *X. laevis*.

(A) Experimental design to compare the fertilization-signaled depolarization in the presence of 1 μM U73122 versus pretreating sperm or eggs with 1 μM U73122 before insemination in control conditions. Blue indicates control solutions, MR/5, and red indicates MR/5 supplemented with 1 μM U73122. For experiments pretreating only sperm, testes were macerated and incubated in 1 μM U73122 for 10 min and applied to untreated eggs in MR/5. For experiments pretreating only eggs, eggs were incubated for 10 min in 1 μM U73122 and inseminated in MR/5 with untreated sperm. (B) Representative whole-cell fertilization recording using sperm pretreated with 1 μM U73122. The gray dashed line denotes zero mV. Tukey box plot distributions of (C) resting and fertilization membrane potentials and (D) depolarization rate in control conditions and U73122 pretreated sperm. The middle line denotes the median value, the box indicates 25-75%, and the whiskers represent 10-90% of the data distribution. (E) Representative whole-cell fertilization recording from an egg pretreated with U73122. Blue arrows denote multiple sperm additions. (F) Tukey box plot distribution of resting membrane potentials from control and U73122 pretreated eggs. The middle line denotes the median value, the box indicates 25-75%, and the whiskers represent 10-90% of the data distribution.

By contrast, when *X. laevis* eggs were pretreated with 1 μM U73122 for 10 mins and then inseminated without the drug, fertilization did not evoke a depolarization (Figure 4E). The U73122 pretreated eggs maintained a resting potential that was not significantly different from control condition recordings (-12.8 ± 0.6, N=5, *P*=1.0 vs -13.4 ± 1.0 mV for control, Figure 4F). Moreover, eggs fertilized with pretreated sperm developed symmetric cleavage furrows, while pretreated eggs performed asymmetric cleavage furrows, indicating polyspermic fertilization. Together, these results indicate that the fast block to polyspermy requires the activation of an egg-derived PLC during fertilization.

3.4 *X. laevis* eggs have three PLC candidates for triggering the fast block

To determine how fertilization activates PLC to signal the fast block, I first sought to identify which PLC isoforms are present in *X. laevis* eggs. I examined two previously published *X. laevis* expression datasets – the proteome of fertilization-competent eggs (Wuhr et al., 2014) and the RNA-sequencing dataset acquired during different stages of development of *X. laevis* oocytes and eggs (Session et al., 2016). I queried for all proteins encoded by known PLC genes (Figure 5) and found that three PLC proteins are present in the egg: PLCγ1 (encoded by the PLCG1 gene), PLCβ1 and PLCβ3 (encoded by the PLCB1 and PLCB3 genes, respectively). The most abundant PLC in the *X. laevis* egg, PLCγ1, is present at 85.2 nM, an approximately 20-fold higher concentration than either PLCβ1 (3.9 nM), or PLCβ3 (4.3 nM). As a control, I examined the RNA-sequencing dataset with the reasoning that if PLCγ1, PLCβ1, and PLCβ3 proteins are present in the fertilization-competent eggs, the RNA encoding these enzymes ought to be present in the developing gamete. Indeed, the RNA for all three PLC isoforms was present in the developing

oocytes and fertilization-competent egg (Figure 5). The mRNA encoding PLC isoforms not found in the proteome of the egg were also present (Figure 5); this is expected as the mature, unfertilized egg contains the RNA necessary for the divisions to reach the first 4,000 cells when the maternal-to-zygotic transition occurs during *X. laevis* development (Yang et al., 2015). To determine the method of activation for the PLC used during the fast block to polyspermy in *X. laevis*, I inhibited the canonical signaling pathways that activate the three candidate PLCs, starting with the most abundant, PLCγ1.

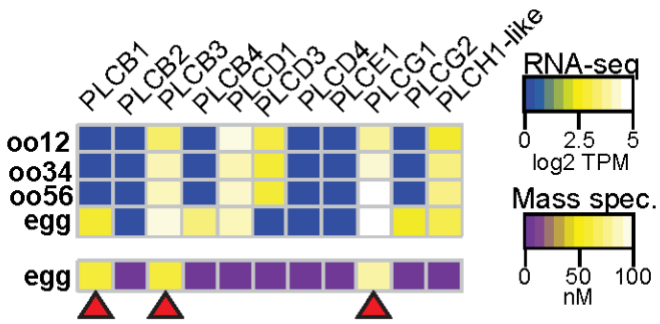

Figure 6: *X. laevis* eggs contain three PLC subtypes.

Heatmaps of PLC subtype RNA (top) and protein (bottom) expression levels in developing *X. laevis* oocytes and eggs. Transcript levels were obtained and compiled from Sessions (Session et al., 2016), and protein concentrations were from Wühr (Wuhr et al., 2014) through mass spectrometry. RNA-seq data is displayed as transcripts per million (TPM), and protein is shown as nanomolar concentration. Red arrows indicate PLC subtypes present in both RNA sequencing and mass spectrometry datasets in unfertilized *X. laevis* eggs. Oo12, oo34, and oo56 indicate different developmental stages in *X. laevis* oocytes.

3.5 Tyrosine phosphorylation of PLCγ1 does not signal the fast block

PLCγ1 is typically activated by phosphorylation of the critical tyrosine Y776 (homologous to Y783 in mouse PLCγ1) (Kadamur & Ross, 2013), which resides in the SH2 domain of the

enzyme (Figure 6A). Although PLCγ1-specific inhibitors do not currently exist, I can stop the activation of this PLCγ1 using tyrosine kinase inhibitors. I screened for the efficacy of three inhibitors by assaying *X. laevis* oocytes using Western blots probing specifically for phosphorylated PLCγ1 at Y776; the residue required to be phosphorylated for activation. For these experiments, I exogenously expressed platelet-derived growth factor receptor (PDGF-R), a receptor tyrosine kinase, in *X. laevis* oocytes. Activation of PDGF-R with PDGF application signals the phosphorylation of PLCγ1 at the critical tyrosine at position Y776 (Figure 6B). I found that two of the three screened inhibitors effectively stopped the PDGF-induced PLCγ1 phosphorylation: genistein (100 μM) and dasantinib (100 nM), whereas lavendustin A (100 nM) was not effective (Figure 6B).

Following the inhibitor screen, we made whole-cell recordings on *X. laevis* eggs inseminated in the presence of the validated tyrosine kinase inhibitors genistein and dasantinib to determine whether tyrosine phosphorylation of PLCγ1 is required for the fast block. I did not observe any observable differences between fertilization-evoked depolarizations recorded in solutions supplemented with 100 μM genistein (Figure 6C) or 100 nM dasantinib (Figure 6D) and control recordings (Figure 2C). The mean resting potential of eggs in 100 μM genistein was -17.6 ± 1.9 mV (vs -13.4 ± 1.0 mV for control, P=0.82, Tukey HSD test, Figure 6E). The membrane potential following the fertilization-evoked depolarization was 2.4 ± 2.6 mV (vs 3.2 ± 1.8 mV for controls, P=1.0, Tukey HSD test) (N=7-44 eggs in 3 independent trials, Figure 6E). The depolarization rate was also not altered, as the average was 8.9 ± 3.1 mV/ms compared to 6.7 ± 1.9 mV/ms for depolarizations recorded under control conditions (P=1.0, Tukey HSD test, Figure 6F). Eggs recorded during fertilization in 100 nM dasantinib had a mean resting potential of -10.3 ± 2.2 mV (vs -13.4 ± 1.0 mV for control, P=0.96, Tukey HSD test, Figure 6E) and membrane

potential after the fertilization-evoked depolarization of -1.3 ± 1.9 mV (vs 3.2 ± 1.8 mV for controls, *P*=0.94, Tukey HSD test, Figure 6E). The average rate of depolarization for eggs in 100 nM dasantinib was 3.5 ± 1.9 mV/ms (vs 6.7 ± 1.9 mV/ms, *P*=0.99, Tukey HSD test, Figure 6F). Additionally, the eggs fertilized in the presence of dasantinib and genistein were stored for up to 120 minutes to observe the formation of cleavage furrows, an indicator of monospermic or polyspermic fertilization. These eggs exhibited even cleavages, indicative of monospermic fertilization.

Previously published research suggested that when injected into *X. laevis* eggs, lavendustin A stopped the fast block in *X. laevis* fertilization (Glahn, Mark, Behr, & Nuccitelli, 1999). Although lavendustin A did not effectively stop the PDGF-R signaled phosphorylation of PLCγ1 Y773 (Figure 6B), we made whole-cell recordings from *X. laevis* eggs in the presence of 100 nM lavendustin A or its inactive analog lavendustin B. I observed similar resting potentials, -7.9 ± 2.4 mV and -8.1 ± 2.5 mV, fertilization potentials, 19.7 ± 3.9 mV and 19.8 ± 3.8 mV, and depolarization rates, 0.7 ± 0.5 mV/ms and 0.3 ± 0.2 mV/ms, which were not significantly different from control rates. The occurrence of normal fertilization-evoked depolarizations of eggs inseminated lavendustin A or B indicate that the inhibitor and inactive analog did not disrupt the fast block to polyspermy in *X. laevis* eggs.

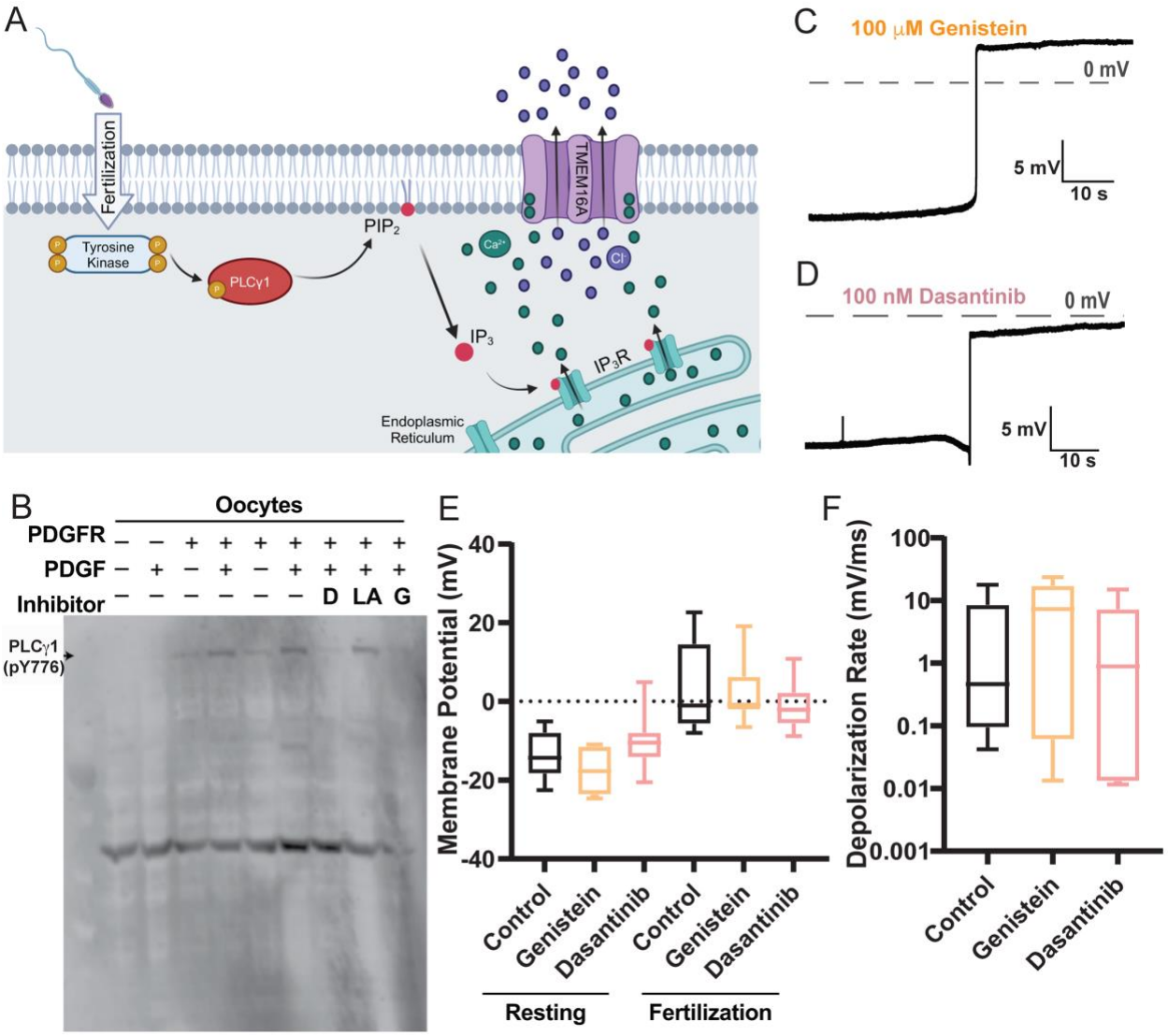

Figure 7: Tyrosine phosphorylation of PLCγ1 is not required for the fast block in *X. laevis*.

(A) A schematic of the tested pathway shows where fertilization activates PLCγ1 by tyrosine kinase phosphorylation. (B) Western blots probing for tyrosine phosphorylation of PLCγ1-Y776 in *X. laevis* oocytes expressing platelet-derived growth factor receptor (PDGFR) in the presence of tyrosine kinase inhibitors (G: Genistein, LA: Lavendustin A, D: Dasantinib) (right) along with PDGFR-expressing and PDGF-activated oocyte controls (left). Oocytes were processed for western blots which revealed that genistein and dasantinib prevented tyrosine phosphorylation of PLCγ1. Representative whole-cell fertilization recordings made in (C) 100 μM genistein or (D) 100 nM dasantinib. The gray dashed line denotes zero mV. Tukey box plot distributions of (E) resting and fertilization membrane potentials in control conditions, genistein, and dasantinib and (F)

depolarization rates in control conditions, genistein, and dasantinib. The middle line denotes the median value, the box indicates 25-75%, and the whiskers represent 10-90% of the data distribution.

To test whether fertilization leads to the phosphorylation of PLCγ1 at the critical tyrosine residue, I also blotted for Y776 phosphorylation in *X. laevis* zygotes shortly after fertilization. For these experiments, *X. laevis* eggs were incubated for 5 min in either control MR/3 conditions or three known tyrosine kinase inhibitors and an inactive analog (genistein, lavendustin A, lavendustin B, or dasantinib) prior to sperm addition. 10 mins following insemination, a timeframe in which the fast block occurs, I removed the jelly surrounding fertilized *X. laevis* eggs that had a contracted animal pole, an indicator that the egg was activated via sperm application. Following jelly removal, zygotes were lysed and processed for western blots as described previously, and in 3 independent trials, I observed no evidence of PLCγ1 Y776 phosphorylation (Figure 7). Within the same western blot, as a control, I included samples of PDGFR-expressing *X. laevis* oocytes and saw phosphorylation of PLCγ1 of Y776 to ensure antibody validity in the blot (Figure 7). Altogether, my results demonstrate that PLCγ1 is not activated by tyrosine phosphorylation during *X. laevis* fertilization.

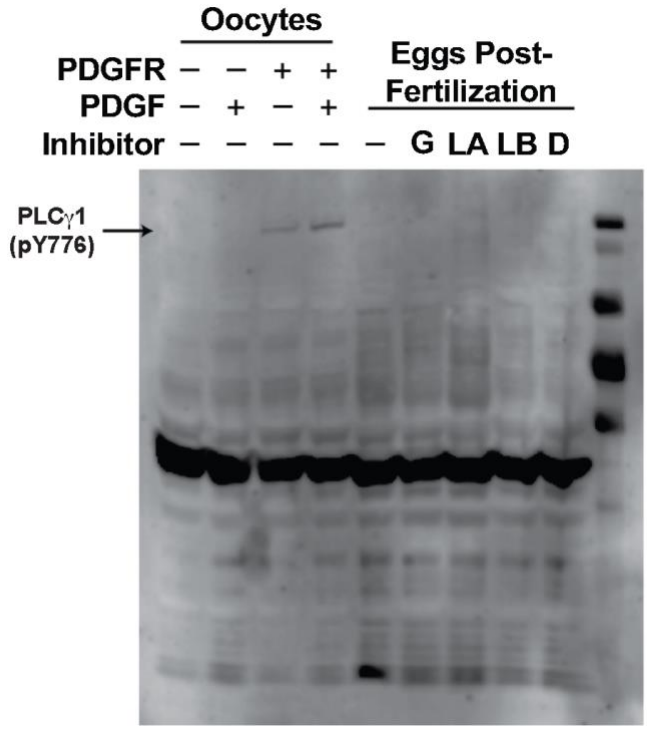

Figure 8: Fertilization did not trigger phosphorylation of Y776 of PLCγ1 in *X. laevis*.

Western blot probing for tyrosine phosphorylation of PLCγ1-Y776 in *X. laevis* oocytes with PDGFR-expressing and PDGF-activated oocyte controls (left) and fertilized *X. laevis* eggs in the presence of screened tyrosine kinase inhibitors (G: Genistein, LA: Lavendustin A, LB: Lavendustin B, or D: Dasantinib).

3.6 $G\alpha_{11}$ activation of PLCβ is not required for the fast block in *X. laevis*

Next, I investigated whether the activation of the two other PLCβ isoforms, PLCβ1 and PLCβ3, is required to signal the fast block (Figure 5). PLCβ isoforms are typically activated by G-protein coupled pathways mediated by the $G\alpha_q$ family (Rhee, Suh, Ryu, & Lee, 1989; Smrcka, Hepler, Brown, & Sternweis, 1991). The $G\alpha_q$ family is comprised of four members, all capable of activating PLCβ: $G\alpha_q$, $G\alpha_{11}$, $G\alpha_{14}$, and $G\alpha_{15}$ (Peavy et al., 2005). To determine which Gα family members are expressed in *X. laevis* eggs, I again referenced the proteomics (Wuhr et al., 2014) and RNAseq (Session et al., 2016) datasets for *X. laevis* eggs. Of the four Gα subtypes (genes: GNA11, GNA14, GNA15, and GNAQ), I found that only protein for GNA11 was present in the unfertilized *X. laevis* eggs (Figure 8A). This indicated that a $G\alpha_{11}$-mediated signaling pathway could activate PLCβ for the fast block.

To test whether $G\alpha_{11}$ signaling is required for the fast block, I first sought to identify inhibitors that stop $G\alpha_{11}$ activation of PLCβ. To do so, I utilized the two-electrode voltage clamp technique (Figure 8B) to record from *X. laevis* oocytes expressing the chimeric light-activated muscarinic receptor, opto-M1R (Morri et al., 2018). Opto-M1R is a chimera between two G protein-coupled receptors: the light-activated rhodopsin and the muscarinic receptor. This receptor maintains the opsin and transmembrane domains of rhodopsin, with the intracellular loops of the muscarinic receptor, thereby enabling the Opto-M1R chimera to be activated by blue/green light, but then activate the same intracellular signaling pathway of the muscarinic receptor which includes activation PLCβ via $G\alpha_{q/11}$. Expressing Opto-M1R in *X. laevis* oocytes enabled me to apply light to these cells to signal an IP_3-mediated Ca^{2+} release from the ER (Figure 8C). The increase of intracellular Ca^{2+} then activates TMEM16A channels, which I experimentally observed

with two-electrode voltage clamp. For these experiments, I recorded from opto-M1R-expressing *X. laevis* oocytes clamped at -80 mV before and after blue/green light application. I first established that under control conditions, repeated light applications evoked similar amplitudes of TMEM16A conducted currents (Figure 8D).

I then screened known $G\alpha_{q/11}$ inhibitors YM-254890 (Figure 8E) (Uemura et al., 2006) and BIM-46187 (Figure 8G) (Schmitz et al., 2014) by comparing TMEM16A conducted currents before or during the application of the inhibitors. After an initial light application in control conditions, Opto-M1R expressing oocytes were exposed to a second light application following a 10 min incubation in the presence of either inhibitor. I found that YM-254890 significantly reduced Opto-M1R-induced activation of TMEM16A channels, with the remaining current following the second light application reduced from an average of 108 ± 9.9% remaining current under control conditions (N=8) to 16 ± 4.9% remaining current in 10 μM YM-254890 (N=5, P=0.05, Figure 8F). BIM-46187, however, did not alter the Opto-M1R signaled activation of TMEM16A conducted current via opto-M1R induction, with 103 ± 17% remaining current in 25 μM BIM-46187 (Figure 8F). These data indicate that YM-254890 effectively stopped $G\alpha_{11}$ activation of PLCβ.

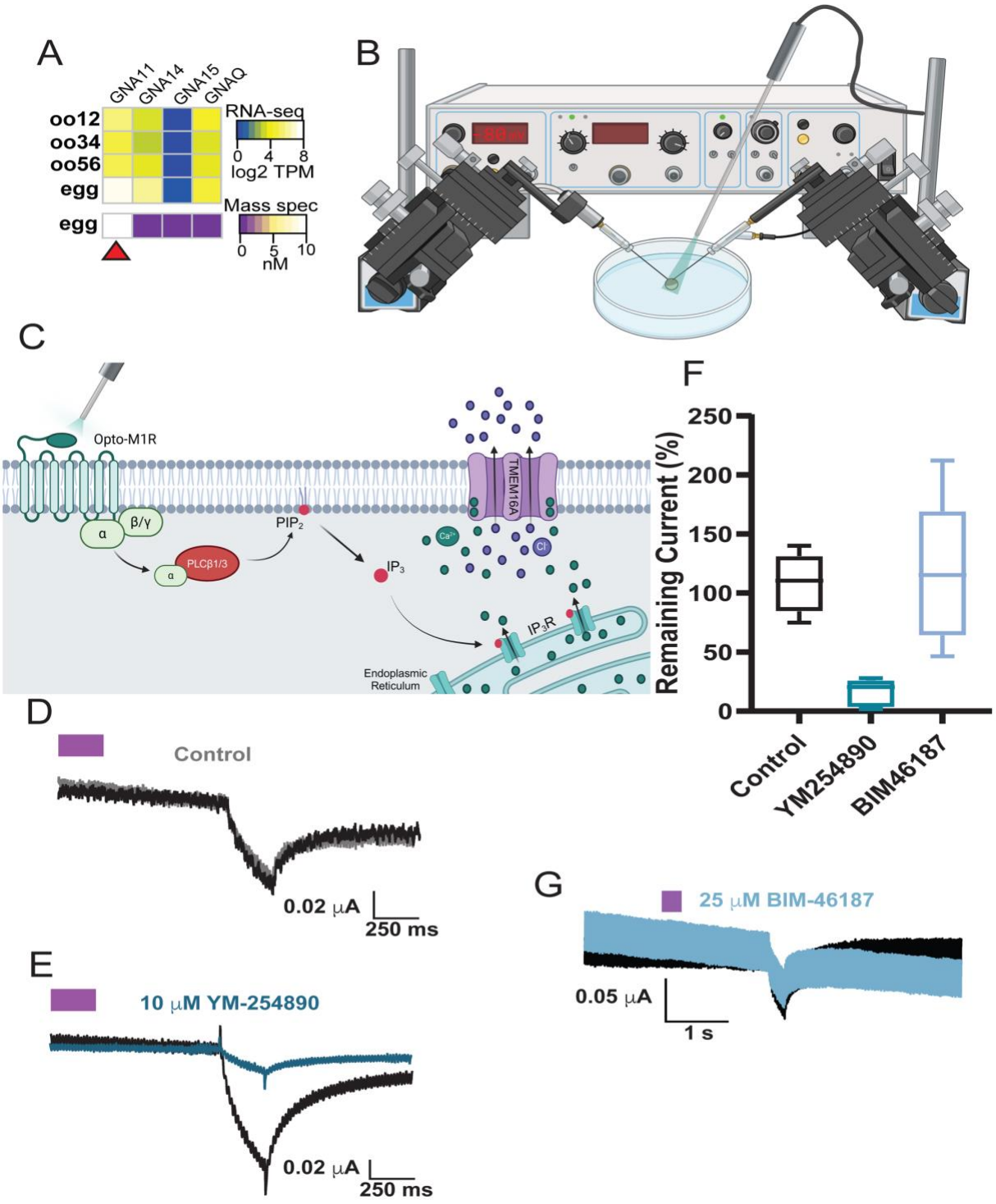

Figure 9: Screening $G\alpha_{q/11}$ inhibitor efficacy in *X. laevis* oocytes.

(A) Heatmaps of $G\alpha_q$ family isoform RNA (top) and protein (bottom) expression levels in developing *X. laevis* oocytes and eggs. Transcript levels were obtained and compiled from Sessions (Session et al., 2016), and protein concentrations were from Wühr (Wuhr et al., 2014) through mass spectrometry. RNA-seq

data is displayed as transcripts per million (TPM), and protein data is shown in nanomolar concentration. The red arrow indicates that the $G\alpha_{11}$ subtype (encoded by GNA11) is present in both RNA sequencing and mass spectrometry datasets in *X. laevis* eggs was observed in mature eggs. (B) Two-electrode voltage clamp (TEVC) recording set up was used to screen inhibitor efficacy on *X. laevis* oocytes clamped at -80 mV. Two electrodes impale the oocyte and measure the current with 250 ms application of blue-green light. (C) Schematic of PLCβ1/3 activation using opto-M1R expression in *X. laevis* oocytes. Representative TEVC recording in control (D) conditions in oocytes expressing opto-M1R and clamped at -80 mV and before and after a 10-minute incubation in 10 μM YM-254890, a $G\alpha_{11/q}$ inhibitor (E). The purple bar denotes the 250 ms blue-green light application. (F) Tukey box plot distributions of the percent remaining current in consecutive recordings in control, 10 μM YM-254890, or 25 μM BIM-46187 conditions from oocytes expressing opto-M1R. The middle line indicates the median value while the box denotes 25-75% and the whiskers 10-90% values of the data distribution. (G) Representative consecutive TEVC recordings before and after a 10 min incubation in 25 μM BIM-46187 clamped at -80 mV.

I then tested whether $G\alpha_{11}$ activation of PLCβ signals the fast block during X. laevis fertilization by inhibiting this pathway with YM-254890 (Figure 9A). To do so, I performed whole-cell recordings on *X. laevis* eggs during fertilization, following a 10 min incubation in the presence of 10 μM YM-254890. I observed normal fertilization-evoked depolarizations in six independent trials in the presence of 10 μM YM-254890, as shown in an example recording in Figure 9B. The eggs inseminated in 10 μM YM-254890 had average resting potentials of -9.3 ± 1.9 mV before (vs -13.4 ± 1.0 mV from control recordings, P=0.92, Tukey HSD), and 0.5 ± 1.3 mV (vs 3.2 ± 1.8 mV/ms, P= 1.0, Tukey HSD) after the fertilization evoked depolarization (Figure 9C). The depolarization rates were also similar in the presence or absence of YM-254890, with an average 1.1 ± 0.7 mV/ms in the inhibitor compared to 6.7 ± 1.9 mV/ms in control conditions (P=0.92, Tukey HSD, Figure 9D). These results show that fertilization does not require a $G\alpha_{11}$ coupled activation of PLCβ.

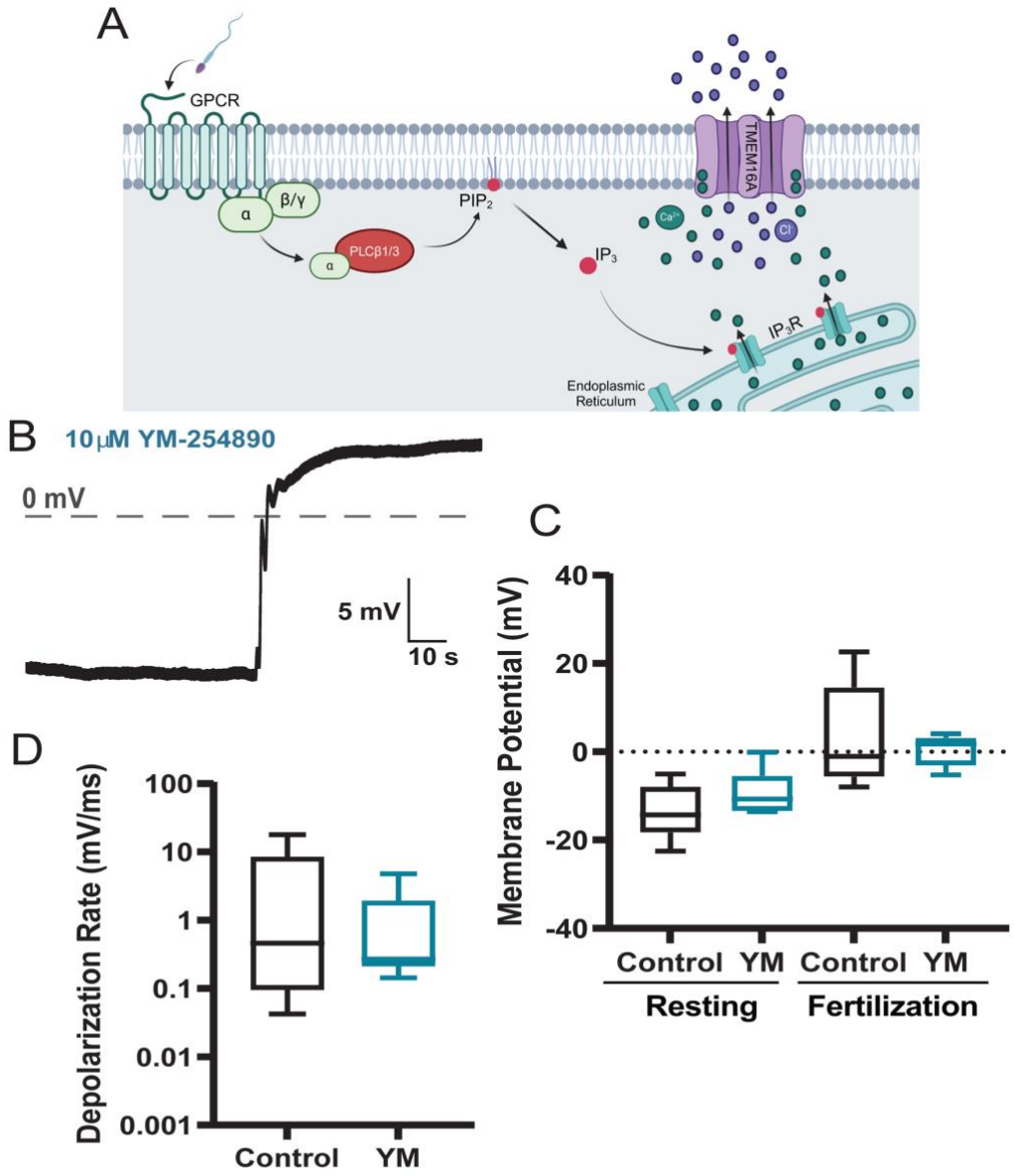

Figure 10: Inhibiting PLCβ1/3 activation via Gα_{11} did not alter the fast block to polyspermy in *X. laevis* eggs. **(A) The schematic depicts a potential activation pathway for PLCβ1/3 via the GPCR subunit Gα_{11}. (B) Representative whole-cell fertilization recording in the presence of 10 μM YM-254890. The gray dashed line denotes zero mV. Tukey box plot distributions of (C) resting and fertilization membrane potentials and (D) depolarization rates in control and YM-254890 conditions. The middle line denotes the median value, the box indicates 25-75%, and the whiskers represent 10-90% of the data distribution.**

4.0 Discussion

4.1 Summary

This dissertation expands our understanding of how fertilization triggers the fast block to polyspermy in the African clawed frog, *Xenopus laevis*. I have shown that the PLC necessary for the fast block to polyspermy is derived from the egg, not the sperm, and one of three isoforms: PLCγ1, PLCβ1, and PLCβ3. Using whole-cell recordings during fertilization in the presence of inhibitors targeting the signaling pathways that typically activate each isoform, tyrosine kinase for PLCγ and $G\alpha_{11}$ for PLCβ1/3, I have demonstrated that the fast block depolarization was unaffected and that these fertilizations were monospermic. Although my dissertation did not directly identify the signaling pathway that activates PLC for the fast block, my data will serve as the foundation for future experiments testing how fertilization in *X. laevis* turns on the egg PLC.

4.2 The role of tyrosine phosphorylation in PLCγ activation is controversial

My data demonstrates that phosphorylation of the critical tyrosine (Y776) in PLCγ1 is not required for the fast block, which conflicts with other published findings regarding how fertilization in *X. laevis* activates egg PLCs. Studies from Sato and colleagues suggest that *X. laevis* sperm bind the extracellular domain of uroplakin III on eggs to signal activation of a Src family kinase to tyrosine phosphorylate PLCγ, increase intracellular Ca^{2+} and initiate the slow block to polyspermy and embryonic development (Mahbub Hasan et al., 2014; Sato, Tokmakov, Iwasaki,

& Fukami, 2000). This model is based in part on experiments imaging the cytoplasmic Ca^{2+} during fertilization of *X. laevis* eggs that had been injected with lavendustin A or tyrphostin B46. Both lavendustin A and tyrphostin B46 are known tyrosine kinase inhibitors, and following their injection, fertilization did not trigger an elevation of cytoplasmic Ca^{2+} (Glahn et al., 1999). They also reported that utilizing 100 μM genistein to inhibit tyrosine phosphorylation of PLCγ completely prevented embryonic development of *X. laevis* eggs (Sato et al., 1998). Here, however, we found that neither lavendustin A nor genistein altered the fast block. One key difference between our experiments that may give rise to difference in outcomes is that we allowed the inhibitors to diffuse into the egg, whereas they injected the compounds. These chemicals are small, membrane-permeable inhibitors that are the approximate size of an amino acid. Moreover, I used a specific antibody to monitor tyrosine phosphorylation of PLCγ1-Y776, whereas they used a general phosphotyrosine targeting antibody. Finally, my data indicates that fertilization does not turn on PLCγ1 via Y776 phosphorylation.

My data does agree with other published findings by Runft and colleagues, who also imaged cytoplasmic Ca^{2+} in *X. laevis* eggs during fertilization (Runft, Watras, & Jaffe, 1999). They reported that stopping either PLCγ activity by overexpressing the enzyme's SH2 domain or PLCβ activation with a Ga_q targeting antibody did not alter the fertilization-signaled increase in cytoplasmic Ca^{2+} (Runft et al., 1999). These data suggest that neither tyrosine phosphorylation of PLCγ nor Ga_q activation of PLCβ is needed for the fertilization-triggered increase of cytoplasmic Ca^{2+} signals the slow block. Whether this Ca^{2+} wave is quick enough to trigger the fast block is yet to be determined.

4.3 U73122 mechanism is controversial

U73122 is a general PLC inhibitor that stops the enzyme from cleaving PIP_2 into its two secondary messengers, IP_3 and DAG (Bleasdale et al., 1989). Structurally, U73122 is similar to its inactive analog, U73343, with the only difference being the maleimide moiety in U73122 is replaced with a succinimide (Bleasdale et al., 1989). Maleimides covalently bind thiols in reducing conditions such as the intracellular milieu. Although this moiety is the only structural difference between active U73122 and inactive U73343, it is important to note that changes to other parts of U73122's structure also weaken inhibition (Bleasdale et al., 1989; Bleasdale & Fisher, 1993). At the 1 μM concentration, U73122 has been widely used as a PLC inhibitor, including in *X. laevis* eggs (Bleasdale et al., 1989; Bleasdale & Fisher, 1993; Sato et al., 2000; Stith, 2015; Tokmakov, Sato, Iwasaki, & Fukami, 2002; Wozniak, Tembo, et al., 2018). However, at higher concentrations and in non-reducing conditions, 10+ μM U73122 was shown to activate human PLCs (Klein et al., 2011). This finding has led some scientists to question whether U73122 inhibits PLC. However, under these same experimental conditions, this PLC activation was not observed by 1 μM U73122. The lack of a reducing condition in this cuvette assay could account for the variability observed with U73122 at 1 vs 10 μM because maleimides function differently in reducing versus oxidizing conditions (Boyatzis et al., 2017). A wealth of published data suggests that 1 μM U73122 effectively inhibits intracellular PLC. Moreover, other experimental data from our own lab supports a required role of PLC in the fast block, including lack of any fertilization-signaled depolarization in eggs inseminated in the presence of inhibitors of the IP_3 receptor (Wozniak, Tembo, et al., 2018).

4.4 Activation of PLCβ by other pathways in *X. laevis* eggs

In addition to $G\alpha_{q/11}$, the Gβγ complex derived from Ga_i signaling can activate PLCβ subtypes (Boyer et al., 1992). For most cells, $G\alpha_i$ is the highest expressed α subunit and, consequently, the most abundant source of Gβγ signaling (Hepler & Gilman, 1992; Touhara & MacKinnon, 2018); *X. laevis* eggs are no exception as they abundantly express three $G\alpha_i$ isoforms (Session et al., 2016; Wuhr et al., 2014). However, previously published data suggests that this pathway of PLCβ activation did not contribute to the fast polyspermy block and, therefore, was not explored in this dissertation (Kline, Kopf, Muncy, & Jaffe, 1991). Specifically, Kline and colleagues demonstrated that inhibiting $G\alpha_i$ signaling with pertussis toxin did not alter the fertilization signaled depolarization in *X. laevis* eggs (Kline et al., 1991), which would not be the case if the Gβγ subunit activated PLCβ during the fast block.

5.0 Future Studies

5.1 Potential activation mechanisms of PLC during the fast block in *X. laevis*

I propose three mechanisms for how fertilization could activate an egg PLC, each readily testable. First, PLC could be activated directly by Ca^{2+}. In this Ca^{2+}-induced Ca^{2+} release model, fertilization would trigger an increase of egg Ca^{2+} that would then activate PLC to signal the release of more Ca^{2+} and then activate more PLC. This pathway requires that sperm-derived Ca^{2+} is released in the egg to activate PLC. All three PLC subtypes in *X. laevis* eggs, PLCγ1 and PLCβ1/3, can be activated by Ca^{2+} (Hwang, Jhon, Bae, Kim, & Rhee, 1996; Ryu, Suh, Cho, Lee, & Rhee, 1987; Wahl, Jones, Nishibe, Rhee, & Carpenter, 1992). To test this hypothesis, the intracellular Ca^{2+} in *X. laevis* sperm could be chelated with BAPTA-AM, a cell-permeant Ca^{2+} chelator. If sperm release Ca^{2+} to signal the fast block, I expect that fertilization with BAPTA-AM loaded sperm would not signal a depolarization, detectable with whole-cell recordings on *X. laevis* eggs.

Second, fertilization could increase egg PIP_3 to activate PLC. For PIP_3 to turn on PLC to trigger the fast block, fertilization could activate an egg PI 3-kinase, which would make PIP_3, sperm could enter the egg and release PIP_3, or sperm could be providing a PI 3-kinase that phosphorylates PIP_2 in the egg to make PIP_3 during egg fusion. PIP_3 activates PLCγ1 by interacting with either of the PH domains in the enzyme (Falasca et al., 1998). Once PLCγ1 is activated by PIP_3, PIP_3 also functions as an anchor for PLCγ1 to the membrane, bringing it in closer proximity to its substrate in the membrane, which could lend to the efficiency of the fast block (Kim, Kim, Ryu, & Suh, 2000). To determine if fertilization activates a PI 3-kinase to increase PIP_3 and turn on PLC, whole-cell recordings could be made on *X. laevis* eggs during fertilization in the presence

of PI 3-kinase inhibitors, such as Wortmannin (Wymann et al., 1996) or LY294002 (El-Kholy et al., 2003). Because Wortmannin covalently modifies PI 3-kinases (Norman et al., 1996), sperm and egg could be separately pretreated and used in fertilization experiments to determine if an egg or sperm-derived PI 3-kinase is important for the fast block in *X. laevis.* Finding that fertilization does not signal a depolarization in the presence of a PI 3-kinase inhibitor would suggest that PIP_3 may activate PLC to signal the fast block to polyspermy. In this event, I also predict that these embryos would develop asymmetric cleavage furrows to indicate polyspermic fertilizations.

Finally, phosphatidic acid (PA) could activate PLC to signal the fast block. This hypothesis is based on the finding that fertilization increases the PA content of *X. laevis* eggs (Bates et al., 2014), and that PA has been shown to activate PLCβ (Litosch, 2003) and PLCγ1 (Jones & Carpenter, 1993). PA is generated by the enzyme phospholipase D (PLD), thus, to test if the fast block requires PA to activate PLCβ or PLCγ1, whole-cell fertilization recordings could be made in known PLD inhibitors such as FIPI (Su et al., 2009) and VU0155069 (Scott et al., 2009). If PA is required to activate PLCβ or PLCγ1 during the fast block, inhibiting PLD should abolish the fast block and polyspermic fertilization should be observed.

5.2 How does depolarization of the egg membrane stop sperm entry?

As discussed in the introduction of this dissertation, cross-species fertilization demonstrate sperm somehow detect the membrane potential of the egg (Charbonneau et al., 1983; L. A. Jaffe, Cross, et al., 1983) and that a depolarized membrane in the egg is sufficient to stop sperm entry. In order to explore how sperm sense the membrane potential of eggs, one could test whether the membrane potential of *X. laevis* sperm changes with the membrane potential of bound eggs. To

test this, *X. laevis* sperm could be loaded with fluorescent voltage sensing probes (Adams & Levin, 2012) and confocal microscopy could be used to determine whether *X. laevis* sperm change their membrane potential when bound to depolarized eggs. For these experiments, two-electrode voltage clamp on *X. laevis* eggs, would be used to change their membrane potential. A fluorescence approach would be more straightforward because *X. laevis* sperm are not amenable to electrical recordings. Two electrode voltage clamping on the egg would enable the membrane potential to reach potentials typically seen during the fast block.

Finding that the membrane potential of sperm changes with the membrane potential of eggs could support a potential role for the sperm-expressed voltage-sensing phosphatases (VSPs) in sperm keeping themselves out of depolarized eggs. VSPs reside in the inner acrosomal membrane of sperm from externally fertilizing animals including *X. laevis.* VSPs are enzymes whose activity is altered by the membrane potential. Notably, VSPs are activated by membrane potentials that overlap with the membrane potentials achieved during a fertilization depolarization in *X. laevis* (Ratzan, Evsikov, Okamura, & Jaffe, 2011). If VSPs are responsible for mediating the blockage of additional sperm, the membrane potential of the sperm bound to the egg must vary with the egg's membrane potential.

6.0 Significance and Broader Implications

My dissertation research sought to uncover the signaling pathway that activates PLC to trigger the fast block in *X. laevis* fertilization. The experiments in this dissertation provide additional knowledge about pathways that are essential for proper fertilization and embryonic development. Future research to understand how the fast block protects the nascent zygote will improve our knowledge surrounding fertilization and development and lead to further hypotheses about mutations that lead to polyspermic fertilization in monospermic organisms. Knowing more about these processes can also inform conservation strategies targeting vulnerable species like the amphibians used in this research. Additionally, the pathway studied here leads to the activation of TMEM16A, a Ca^{2+}-activated Cl^- channel that plays a significant role in human diseases such as hypertension, asthma, heart disease, and cancer (Duran & Hartzell, 2011). *Xenopus* TMEM16A and mammalian TMEM16A are highly conserved (82.2% identity between *X. laevis* and mouse TMEM16A) (Schroeder et al., 2008; Tembo et al., 2022), which provides a perfect opportunity to study the channel in a native setting and pathway of activation. Understanding more about how TMEM16A is regulated in *X. laevis* could lead to additional knowledge about the regulatory mechanisms of TMEM16A in mammals, such as humans.

Appendix A Appendices and Supplemental Content

Appendix A.1 Tables

Appendix Figure 1

Inhibitors

Inhibitors	Inhibition of	Concentration used	Citation
U73122	General PLC	1 μM	(Bleasdale et al., 1989; Bleasdale & Fisher, 1993)
Genistein	Tyrosine kinases	100 μM	(Akiyama et al., 1987; Akiyama & Ogawara, 1991)
Dasantinib	Tyrosine kinases	100 nM	(Fauziya et al., 2023)
Lavendustin A/B	Tyrosine kinases/ Inactive analog	100 nM	(Glahn et al., 1999; Hsu et al., 1991; Onoda et al., 1989)
YM-254890	$G\alpha_{q/11}$	10 μM	(Uemura et al., 2006)
BIM-46187	$G\alpha_{q/11}$	25 μM	(Schmitz et al., 2014)

.

Bibliography

Adams, D. S., & Levin, M. (2012). Measuring resting membrane potential using the fluorescent voltage reporters DiBAC4(3) and CC2-DMPE. *Cold Spring Harb Protoc, 2012*(4), 459-464. doi:10.1101/pdb.prot067702

Akiyama, T., Ishida, J., Nakagawa, S., Ogawara, H., Watanabe, S., Itoh, N., . . . Fukami, Y. (1987). Genistein, a specific inhibitor of tyrosine-specific protein kinases. *J Biol Chem, 262*(12), 5592-5595. Retrieved from https://www.ncbi.nlm.nih.gov/pubmed/3106339

Akiyama, T., & Ogawara, H. (1991). Use and specificity of genistein as inhibitor of protein-tyrosine kinases. *Methods Enzymol, 201*, 362-370. doi:10.1016/0076-6879(91)01032-w

al-Anzi, B., & Chandler, D. E. (1998). A sperm chemoattractant is released from Xenopus egg jelly during spawning. *Dev Biol, 198*(2), 366-375. Retrieved from https://www.ncbi.nlm.nih.gov/pubmed/9659939

Alberts, B. (2002). Molecular biology of the cell. In (4th ed., pp. xxxiv, 1463, 1486 p.). New York: Garland Science.

Bae, Y. S., Cantley, L. G., Chen, C. S., Kim, S. R., Kwon, K. S., & Rhee, S. G. (1998). Activation of phospholipase C-gamma by phosphatidylinositol 3,4,5-trisphosphate. *J Biol Chem, 273*(8), 4465-4469. doi:10.1074/jbc.273.8.4465

Bainbridge, R. E., Rosenbaum, J. C., Sau, P., & Carlson, A. E. (2023). Xenopus laevis lack the critical sperm factor PLCzeta. *bioRxiv*. doi:10.1101/2023.02.02.526858

Bates, R. C., Fees, C. P., Holland, W. L., Winger, C. C., Batbayar, K., Ancar, R., . . . Stith, B. J. (2014). Activation of Src and release of intracellular calcium by phosphatidic acid during Xenopus laevis fertilization. *Dev Biol, 386*(1), 165-180. doi:10.1016/j.ydbio.2013.11.006

Berg, L. K., & Wessel, G. M. (1997). Cortical granules of the sea urchin translocate early in oocyte maturation. *Development, 124*(9), 1845-1850. doi:10.1242/dev.124.9.1845

Bianchi, E., & Wright, G. J. (2016). Sperm Meets Egg: The Genetics of Mammalian Fertilization. *Annu Rev Genet, 50*, 93-111. doi:10.1146/annurev-genet-121415-121834

Bill, C. A., & Vines, C. M. (2020). Phospholipase C. *Adv Exp Med Biol, 1131*, 215-242. doi:10.1007/978-3-030-12457-1_9

Bleasdale, J. E., Bundy, G. L., Bunting, S., Fitzpatrick, F. A., Huff, R. M., Sun, F. F., & Pike, J. E. (1989). Inhibition of phospholipase C dependent processes by U-73, 122. *Adv Prostaglandin Thromboxane Leukot Res, 19*, 590-593. Retrieved from https://www.ncbi.nlm.nih.gov/pubmed/2526542

Bleasdale, J. E., & Fisher, S. K. (1993). Use of U73122 as an Inhibitor of Phoapholipase C-Dependent Processes. *Neuroprotocols, 3*(2), 9. doi:https://doi.org/10.1006/ncmn.1993.1046

Boguski, M. S., & McCormick, F. (1993). Proteins regulating Ras and its relatives. *Nature, 366*(6456), 643-654. doi:10.1038/366643a0

Boyatzis, A. E., Bringans, S. D., Piggott, M. J., Duong, M. N., Lipscombe, R. J., & Arthur, P. G. (2017). Limiting the Hydrolysis and Oxidation of Maleimide-Peptide Adducts Improves Detection of Protein Thiol Oxidation. *J Proteome Res, 16*(5), 2004-2015. doi:10.1021/acs.jproteome.6b01060

Boyer, J. L., Waldo, G. L., & Harden, T. K. (1992). Beta gamma-subunit activation of G-protein-regulated phospholipase C. *J Biol Chem, 267*(35), 25451-25456. Retrieved from https://www.ncbi.nlm.nih.gov/pubmed/1460039

Brugnoli, F., Grassilli, S., Lanuti, P., Marchisio, M., Al-Qassab, Y., Vezzali, F., . . . Bertagnolo, V. (2017). Up-modulation of PLC-beta2 reduces the number and malignancy of triple-negative breast tumor cells with a CD133(+)/EpCAM(+) phenotype: a promising target for preventing progression of TNBC. *BMC Cancer, 17*(1), 617. doi:10.1186/s12885-017-3592-y

Burnett, L. A., Sugiyama, H., Bieber, A. L., & Chandler, D. E. (2011). Egg jelly proteins stimulate directed motility in Xenopus laevis sperm. *Mol Reprod Dev, 78*(6), 450-462. doi:10.1002/mrd.21325

Burnett, L. A., Xiang, X., Bieber, A. L., & Chandler, D. E. (2008). Crisp proteins and sperm chemotaxis: discovery in amphibians and explorations in mammals. *Int J Dev Biol, 52*(5-6), 489-501. doi:10.1387/ijdb.072545lb

Busa, W. B., Ferguson, J. E., Joseph, S. K., Williamson, J. R., & Nuccitelli, R. (1985). Activation of frog (Xenopus laevis) eggs by inositol trisphosphate. I. Characterization of Ca2+ release from intracellular stores. *J Cell Biol, 101*(2), 677-682. doi:10.1083/jcb.101.2.677

Camps, M., Carozzi, A., Schnabel, P., Scheer, A., Parker, P. J., & Gierschik, P. (1992). Isozyme-selective stimulation of phospholipase C-beta 2 by G protein beta gamma-subunits. *Nature, 360*(6405), 684-686. doi:10.1038/360684a0

Charbonneau, M., Moreau, M., Picheral, B., Vilain, J. P., & Guerrier, P. (1983). Fertilization of amphibian eggs: a comparison of electrical responses between anurans and urodeles. *Dev Biol, 98*(2), 304-318. doi:10.1016/0012-1606(83)90361-5

Clark, N. L., Aagaard, J. E., & Swanson, W. J. (2006). Evolution of reproductive proteins from animals and plants. *Reproduction, 131*(1), 11-22. doi:10.1530/rep.1.00357

Coy, P., Garcia-Vazquez, F. A., Visconti, P. E., & Aviles, M. (2012). Roles of the oviduct in mammalian fertilization. *Reproduction, 144*(6), 649-660. doi:10.1530/REP-12-0279

Cross, N. L. (1981). Initiation of the activation potential by an increase in intracellular calcium in eggs of the frog, Rana pipiens. *Dev Biol, 85*(2), 380-384. doi:10.1016/0012-1606(81)90269-4

Cross, N. L., & Elinson, R. P. (1980). A fast block to polyspermy in frogs mediated by changes in the membrane potential. *Dev Biol, 75*(1), 187-198. doi:10.1016/0012-1606(80)90154-2

Deneke, V. E., Blaha, A., Lu, Y., Draper, J. M., Phan, C. S., Panser, K., . . . Pauli, A. (2023). A conserved fertilization complex of Izumo1, Spaca6, and Tmem81 mediates sperm-egg interaction in vertebrates. *bioRxiv*, 2023.2007.2027.550750. doi:10.1101/2023.07.27.550750

Deneke, V. E., & Pauli, A. (2021). The Fertilization Enigma: How Sperm and Egg Fuse. *Annu Rev Cell Dev Biol, 37*, 391-414. doi:10.1146/annurev-cellbio-120219-021751

Duran, C., & Hartzell, H. C. (2011). Physiological roles and diseases of Tmem16/Anoctamin proteins: are they all chloride channels? *Acta Pharmacol Sin, 32*(6), 685-692. doi:10.1038/aps.2011.48

El-Kholy, W., Macdonald, P. E., Lin, J. H., Wang, J., Fox, J. M., Light, P. E., . . . Wheeler, M. B. (2003). The phosphatidylinositol 3-kinase inhibitor LY294002 potently blocks K(V) currents via a direct mechanism. *FASEB J, 17*(6), 720-722. doi:10.1096/fj.02-0802fje

Elinson, R. P. (1975). Site of sperm entry and a cortical contraction associated with egg activation in the frog Rana pipiens. *Dev Biol, 47*(2), 257-268. doi:10.1016/0012-1606(75)90281-x

Elinson, R. P. (1986). Fertilization in amphibians: the ancestry of the block to polyspermy. *Int Rev Cytol, 101*, 59-100. doi:10.1016/s0074-7696(08)60246-6

Falasca, M., Logan, S. K., Lehto, V. P., Baccante, G., Lemmon, M. A., & Schlessinger, J. (1998). Activation of phospholipase C gamma by PI 3-kinase-induced PH domain-mediated membrane targeting. *EMBO J, 17*(2), 414-422. doi:10.1093/emboj/17.2.414

Fauziya, Gupta, A., Nadaf, A., Ahmad, S., Hasan, N., Imran, M., . . . Ahmad, F. J. (2023). Dasatinib: a potential tyrosine kinase inhibitor to fight against multiple cancer malignancies. *Med Oncol, 40*(6), 173. doi:10.1007/s12032-023-02018-5

Fisher, I. J., Jenkins, M. L., Tall, G. G., Burke, J. E., & Smrcka, A. V. (2020). Activation of Phospholipase C beta by Gbetagamma and Galpha(q) Involves C-Terminal Rearrangement to Release Autoinhibition. *Structure, 28*(7), 810-819 e815. doi:10.1016/j.str.2020.04.012

Fontanilla, R. A., & Nuccitelli, R. (1998). Characterization of the sperm-induced calcium wave in Xenopus eggs using confocal microscopy. *Biophys J, 75*(4), 2079-2087. doi:10.1016/S0006-3495(98)77650-7

Fukami, K., Nakao, K., Inoue, T., Kataoka, Y., Kurokawa, M., Fissore, R. A., . . . Takenawa, T. (2001). Requirement of phospholipase Cdelta4 for the zona pellucida-induced acrosome reaction. *Science, 292*(5518), 920-923. doi:10.1126/science.1059042

Fukami, K., Yoshida, M., Inoue, T., Kurokawa, M., Fissore, R. A., Yoshida, N., . . . Takenawa, T. (2003). Phospholipase Cdelta4 is required for Ca2+ mobilization essential for acrosome reaction in sperm. *J Cell Biol, 161*(1), 79-88. doi:10.1083/jcb.200210057

Gagoski, D., Polinkovsky, M. E., Mureev, S., Kunert, A., Johnston, W., Gambin, Y., & Alexandrov, K. (2016). Performance benchmarking of four cell-free protein expression systems. *Biotechnol Bioeng, 113*(2), 292-300. doi:10.1002/bit.25814

Gilbert, S. F. (2003). *Developmental biology* (7th ed.). Sunderland, Mass.: Sinauer Associates.

Gilbert, S. F., & Barresi, M. J. F. (2020). Vitelline envelope. In *Developmental biology* (Twelfth edition. ed., pp. 220-221). New York, NY: Oxford University Press.

Glahn, D., Mark, S. D., Behr, R. K., & Nuccitelli, R. (1999). Tyrosine kinase inhibitors block sperm-induced egg activation in Xenopus laevis. *Dev Biol, 205*(1), 171-180. doi:10.1006/dbio.1998.9042

Gresset, A., Hicks, S. N., Harden, T. K., & Sondek, J. (2010). Mechanism of phosphorylation-induced activation of phospholipase C-gamma isozymes. *J Biol Chem, 285*(46), 35836-35847. doi:10.1074/jbc.M110.166512

Gresset, A., Sondek, J., & Harden, T. K. (2012). The phospholipase C isozymes and their regulation. *Subcell Biochem, 58*, 61-94. doi:10.1007/978-94-007-3012-0_3

Grey, R. D., Bastiani, M. J., Webb, D. J., & Schertel, E. R. (1982). An electrical block is required to prevent polyspermy in eggs fertilized by natural mating of Xenopus laevis. *Dev Biol, 89*(2), 475-484. doi:10.1016/0012-1606(82)90335-9

Grey, R. D., Wolf, D. P., & Hedrick, J. L. (1974). Formation and structure of the fertilization envelope in Xenopus laevis. *Dev Biol, 36*(1), 44-61. doi:10.1016/0012-1606(74)90189-4

Hepler, J. R., & Gilman, A. G. (1992). G proteins. *Trends Biochem Sci, 17*(10), 383-387. doi:10.1016/0968-0004(92)90005-t

Hill, W. G., Southern, N. M., MacIver, B., Potter, E., Apodaca, G., Smith, C. P., & Zeidel, M. L. (2005). Isolation and characterization of the Xenopus oocyte plasma membrane: a new method for studying activity of water and solute transporters. *Am J Physiol Renal Physiol, 289*(1), F217-224. doi:10.1152/ajprenal.00022.2005

Hsu, C. Y., Persons, P. E., Spada, A. P., Bednar, R. A., Levitzki, A., & Zilberstein, A. (1991). Kinetic analysis of the inhibition of the epidermal growth factor receptor tyrosine kinase by Lavendustin-A and its analogue. *J Biol Chem, 266*(31), 21105-21112. Retrieved from https://www.ncbi.nlm.nih.gov/pubmed/1939153

Hwang, S. C., Jhon, D. Y., Bae, Y. S., Kim, J. H., & Rhee, S. G. (1996). Activation of phospholipase C-gamma by the concerted action of tau proteins and arachidonic acid. *J Biol Chem, 271*(31), 18342-18349. doi:10.1074/jbc.271.31.18342

Ilkaeva, O., Kinch, L. N., Paulssen, R. H., & Ross, E. M. (2002). Mutations in the carboxyl-terminal domain of phospholipase C-beta 1 delineate the dimer interface and a potential Galphaq interaction site. *J Biol Chem, 277*(6), 4294-4300. doi:10.1074/jbc.M109612200

Iwao, Y. (1989). An electrically mediated block to polyspermy in the primitive urodele Hynobius nebulosus and phylogenetic comparison with other amphibians. *Dev Biol, 134*(2), 438-445. doi:10.1016/0012-1606(89)90116-4

Jaffe, L. A. (1976). Fast block to polyspermy in sea urchin eggs is electrically mediated. *Nature, 261*(5555), 68-71. doi:10.1038/261068a0

Jaffe, L. A., Cross, N. L., & Picheral, B. (1983). Studies of the voltage-dependent polyspermy block using cross-species fertilization of amphibians. *Dev Biol, 98*(2), 319-326. doi:0012-1606(83)90362-7 [pii]

Jaffe, L. A., Sharp, A. P., & Wolf, D. P. (1983). Absence of an electrical polyspermy block in the mouse. *Dev Biol, 96*(2), 317-323. doi:10.1016/0012-1606(83)90168-9

Jaffe, L. F. (1983). Sources of calcium in egg activation: a review and hypothesis. *Dev Biol, 99*(2), 265-276. doi:10.1016/0012-1606(83)90276-2

Jones, G. A., & Carpenter, G. (1993). The regulation of phospholipase C-gamma 1 by phosphatidic acid. Assessment of kinetic parameters. *J Biol Chem, 268*(28), 20845-20850. Retrieved from https://www.ncbi.nlm.nih.gov/pubmed/8407914

Just, E. (1919). The fertilization reaction in Echinarachnius parma: I. Cortical response of the egg to insemination. *The Biological Bulletin, 36*(1), 1-10.

Kadamur, G., & Ross, E. M. (2013). Mammalian phospholipase C. *Annu Rev Physiol, 75*, 127-154. doi:10.1146/annurev-physiol-030212-183750

Kawakami, T., & Xiao, W. (2013). Phospholipase C-beta in immune cells. *Adv Biol Regul, 53*(3), 249-257. doi:10.1016/j.jbior.2013.08.001

Kawakami, T., Xiao, W., Yasudo, H., & Kawakami, Y. (2012). Regulation of proliferation, survival, differentiation, and activation by the Signaling Platform for SHP-1 phosphatase. *Adv Biol Regul, 52*(1), 7-15. doi:10.1016/j.advenzreg.2011.09.003

Kawasaki, H., & Kretsinger, R. H. (1994). Calcium-binding proteins. 1: EF-hands. *Protein Profile, 1*(4), 343-517. Retrieved from https://www.ncbi.nlm.nih.gov/pubmed/8528904

Kim, M. J., Kim, E., Ryu, S. H., & Suh, P. G. (2000). The mechanism of phospholipase C-gamma1 regulation. *Exp Mol Med, 32*(3), 101-109. doi:10.1038/emm.2000.18

Klein, R. R., Bourdon, D. M., Costales, C. L., Wagner, C. D., White, W. L., Williams, J. D., . . . Thakker, D. R. (2011). Direct activation of human phospholipase C by its well known inhibitor u73122. *J Biol Chem, 286*(14), 12407-12416. doi:10.1074/jbc.M110.191783

Kline, D. (1988). Calcium-dependent events at fertilization of the frog egg: injection of a calcium buffer blocks ion channel opening, exocytosis, and formation of pronuclei. *Dev Biol, 126*(2), 346-361. doi:10.1016/0012-1606(88)90145-5

Kline, D., Kopf, G. S., Muncy, L. F., & Jaffe, L. A. (1991). Evidence for the involvement of a pertussis toxin-insensitive G-protein in egg activation of the frog, Xenopus laevis. *Dev Biol, 143*(2), 218-229. doi:10.1016/0012-1606(91)90072-b

Komondor, K. M., Bainbridge, R. E., Sharp, K. G., Iyer, A. R., Rosenbaum, J. C., & Carlson, A. E. (2023). TMEM16A activation for the fast block to polyspermy in the African clawed frog does not require conventional activation of egg PLCs. *J Gen Physiol, 155*(10). doi:10.1085/jgp.202213258

Kouchi, Z., Fukami, K., Shikano, T., Oda, S., Nakamura, Y., Takenawa, T., & Miyazaki, S. (2004). Recombinant phospholipase Czeta has high Ca2+ sensitivity and induces Ca2+ oscillations in mouse eggs. *J Biol Chem, 279*(11), 10408-10412. doi:10.1074/jbc.M313801200

Kouchi, Z., Igarashi, T., Shibayama, N., Inanobe, S., Sakurai, K., Yamaguchi, H., . . . Fukami, K. (2011). Phospholipase Cdelta3 regulates RhoA/Rho kinase signaling and neurite outgrowth. *J Biol Chem, 286*(10), 8459-8471. doi:10.1074/jbc.M110.171223

Kunrath-Lima, M., de Miranda, M. C., Ferreira, A. D. F., Faraco, C. C. F., de Melo, M. I. A., Goes, A. M., . . . Gomes, D. A. (2018). Phospholipase C delta 4 (PLCdelta4) is a nuclear protein involved in cell proliferation and senescence in mesenchymal stromal stem cells. *Cell Signal, 49*, 59-67. doi:10.1016/j.cellsig.2018.05.011

Limatola, N., Chun, J. T., & Santella, L. (2022). Regulation of the Actin Cytoskeleton-Linked Ca(2+) Signaling by Intracellular pH in Fertilized Eggs of Sea Urchin. *Cells, 11*(9). doi:10.3390/cells11091496

Litosch, I. (2003). Regulation of phospholipase C-beta activity by phosphatidic acid: isoform dependence, role of protein kinase C, and G protein subunits. *Biochemistry, 42*(6), 1618-1623. doi:10.1021/bi026414h

Liu, M. (2011). The biology and dynamics of mammalian cortical granules. *Reprod Biol Endocrinol, 9*, 149. doi:10.1186/1477-7827-9-149

Lo Vasco, V. R. (2011). Role of phosphoinositide-specific phospholipase C eta2 in isolated and syndromic mental retardation. *Eur Neurol, 65*(5), 264-269. doi:10.1159/000327307

Lomasney, J. W., Cheng, H. F., Wang, L. P., Kuan, Y., Liu, S., Fesik, S. W., & King, K. (1996). Phosphatidylinositol 4,5-bisphosphate binding to the pleckstrin homology domain of phospholipase C-delta1 enhances enzyme activity. *J Biol Chem, 271*(41), 25316-25326. doi:10.1074/jbc.271.41.25316

Maeno, T. (1959). Electrical characteristics and activation potential of Bufo eggs. *J Gen Physiol, 43*(1), 139-157. doi:10.1085/jgp.43.1.139

Mahbub Hasan, A. K., Hashimoto, A., Maekawa, Y., Matsumoto, T., Kushima, S., Ijiri, T. W., . . . Sato, K. (2014). The egg membrane microdomain-associated uroplakin III-Src system becomes functional during oocyte maturation and is required for bidirectional gamete signaling at fertilization in Xenopus laevis. *Development, 141*(8), 1705-1714. doi:10.1242/dev.105510

McCulloh, D. H., Rexroad, C. E., Jr., & Levitan, H. (1983). Insemination of rabbit eggs is associated with slow depolarization and repetitive diphasic membrane potentials. *Dev Biol, 95*(2), 372-377. doi:10.1016/0012-1606(83)90038-6

Metz, C. (2012). *Biology Of Fertilization V3: The Fertilization Response Of the Egg* (Vol. 3): Elsevier.

Miyazaki, S., & Hirai, S. (1979). Fast polyspermy block and activation potential. Correlated changes during oocyte maturation of a starfish. *Dev Biol, 70*(2), 327-340. doi:10.1016/0012-1606(79)90031-9

Miyazaki, S., & Igusa, Y. (1981). Fertilization potential in golden hamster eggs consists of recurring hyperpolarizations. *Nature, 290*(5808), 702-704. doi:10.1038/290702a0

Miyazaki, S., & Igusa, Y. (1982). Ca-mediated activation of a K current at fertilization of golden hamster eggs. *Proc Natl Acad Sci U S A, 79*(3), 931-935. doi:10.1073/pnas.79.3.931

Mizushima, S. (2017). Fertilization 2: Polyspermic Fertilization. *Adv Exp Med Biol, 1001*, 105-123. doi:10.1007/978-981-10-3975-1_7

Moccia, F., Lim, D., Kyozuka, K., & Santella, L. (2004). NAADP triggers the fertilization potential in starfish oocytes. *Cell Calcium, 36*(6), 515-524. doi:10.1016/j.ceca.2004.05.004

Morri, M., Sanchez-Romero, I., Tichy, A. M., Kainrath, S., Gerrard, E. J., Hirschfeld, P. P., . . . Janovjak, H. (2018). Optical functionalization of human Class A orphan G-protein-coupled receptors. *Nat Commun, 9*(1), 1950. doi:10.1038/s41467-018-04342-1

Nakahara, M., Shimozawa, M., Nakamura, Y., Irino, Y., Morita, M., Kudo, Y., & Fukami, K. (2005). A novel phospholipase C, PLC(eta)2, is a neuron-specific isozyme. *J Biol Chem, 280*(32), 29128-29134. doi:10.1074/jbc.M503817200

Nishio, S., Emori, C., Wiseman, B., Fahrenkamp, D., Dioguardi, E., Zamora-Caballero, S., . . . Jovine, L. (2023). Architecture of the vertebrate egg coat and structural basis of the ZP2 block to polyspermy. *bioRxiv*, 2023.2006.2021.544075. doi:10.1101/2023.06.21.544075

Norman, B. H., Shih, C., Toth, J. E., Ray, J. E., Dodge, J. A., Johnson, D. W., . . . Vlahos, C. J. (1996). Studies on the mechanism of phosphatidylinositol 3-kinase inhibition by wortmannin and related analogs. *J Med Chem, 39*(5), 1106-1111. doi:10.1021/jm950619p

Nuccitelli, R. (1980). The fertilization potential is not necessary for the block to polyspermy or the activation of development in the medaka egg. *Dev Biol, 76*(2), 499-504. doi:10.1016/0012-1606(80)90397-8

Nuccitelli, R., Yim, D. L., & Smart, T. (1993). The sperm-induced Ca2+ wave following fertilization of the Xenopus egg requires the production of Ins(1, 4, 5)P3. *Dev Biol, 158*(1), 200-212. doi:10.1006/dbio.1993.1179

Onoda, T., Iinuma, H., Sasaki, Y., Hamada, M., Isshiki, K., Naganawa, H., . . . Umezawa, K. (1989). Isolation of a novel tyrosine kinase inhibitor, lavendustin A, from Streptomyces griseolavendus. *J Nat Prod, 52*(6), 1252-1257. doi:10.1021/np50066a009

Peavy, R. D., Hubbard, K. B., Lau, A., Fields, R. B., Xu, K., Lee, C. J., . . . Hepler, J. R. (2005). Differential effects of Gq alpha, G14 alpha, and G15 alpha on vascular smooth muscle cell survival and gene expression profiles. *Mol Pharmacol, 67*(6), 2102-2114. doi:10.1124/mol.104.007799

Penna, T. (2022). Lazzaro Spallanzani: pioneer of artificial insemination, multidisciplinary research, and scientific dissemination. *History and Philosophy of Medicine, 4*(4), 7. doi:https://doi.org/10.53388/HPM20221001027

Popovics, P., & Stewart, A. J. (2012). Phospholipase C-eta activity may contribute to Alzheimer's disease-associated calciumopathy. *J Alzheimers Dis, 30*(4), 737-744. doi:10.3233/JAD-2012-120241

Puerta Suarez, J., du Plessis, S. S., & Cardona Maya, W. D. (2018). Spermatozoa: A Historical Perspective. *Int J Fertil Steril, 12*(3), 182-190. doi:10.22074/ijfs.2018.5316

Ratzan, W. J., Evsikov, A. V., Okamura, Y., & Jaffe, L. A. (2011). Voltage sensitive phosphoinositide phosphatases of Xenopus: their tissue distribution and voltage dependence. *J Cell Physiol, 226*(11), 2740-2746. doi:10.1002/jcp.22854

Reinhart, D., Ridgway, J., & Chandler, D. E. (1998). Xenopus laevis fertilisation: analysis of sperm motility in egg jelly using video light microscopy. *Zygote, 6*(2), 173-182. doi:10.1017/s0967199498000100

Rhee, S. G. (2001). Regulation of phosphoinositide-specific phospholipase C. *Annu Rev Biochem, 70*, 281-312. doi:10.1146/annurev.biochem.70.1.281

Rhee, S. G., Suh, P. G., Ryu, S. H., & Lee, S. Y. (1989). Studies of inositol phospholipid-specific phospholipase C. *Science, 244*(4904), 546-550. doi:10.1126/science.2541501

Runft, L. L., Jaffe, L. A., & Mehlmann, L. M. (2002). Egg activation at fertilization: where it all begins. *Dev Biol, 245*(2), 237-254. doi:10.1006/dbio.2002.0600

Runft, L. L., Watras, J., & Jaffe, L. A. (1999). Calcium release at fertilization of Xenopus eggs requires type I IP(3) receptors, but not SH2 domain-mediated activation of PLCgamma or G(q)-mediated activation of PLCbeta. *Dev Biol, 214*(2), 399-411. doi:10.1006/dbio.1999.9415

Ryu, S. H., Suh, P. G., Cho, K. S., Lee, K. Y., & Rhee, S. G. (1987). Bovine brain cytosol contains three immunologically distinct forms of inositolphospholipid-specific phospholipase C. *Proc Natl Acad Sci U S A, 84*(19), 6649-6653. doi:10.1073/pnas.84.19.6649

Sakurai, K., Hirata, M., Yamaguchi, H., Nakamura, Y., & Fukami, K. (2011). Phospholipase Cdelta3 is a novel binding partner of myosin VI and functions as anchoring of myosin VI on plasma membrane. *Adv Enzyme Regul, 51*(1), 171-181. doi:10.1016/j.advenzreg.2010.09.014

Sato, K., Iwasaki, T., Tamaki, I., Aoto, M., Tokmakov, A. A., & Fukami, Y. (1998). Involvement of protein-tyrosine phosphorylation and dephosphorylation in sperm-induced Xenopus egg activation. *FEBS Lett, 424*(1-2), 113-118. doi:10.1016/s0014-5793(98)00123-9

Sato, K., Tokmakov, A. A., Iwasaki, T., & Fukami, Y. (2000). Tyrosine kinase-dependent activation of phospholipase Cgamma is required for calcium transient in Xenopus egg fertilization. *Dev Biol, 224*(2), 453-469. doi:10.1006/dbio.2000.9782

Saunders, C. M., Larman, M. G., Parrington, J., Cox, L. J., Royse, J., Blayney, L. M., . . . Lai, F. A. (2002). PLC zeta: a sperm-specific trigger of Ca(2+) oscillations in eggs and embryo development. *Development, 129*(15), 3533-3544. Retrieved from https://www.ncbi.nlm.nih.gov/pubmed/12117804

Schmitz, A. L., Schrage, R., Gaffal, E., Charpentier, T. H., Wiest, J., Hiltensperger, G., . . . Kostenis, E. (2014). A cell-permeable inhibitor to trap Galphaq proteins in the empty pocket conformation. *Chem Biol, 21*(7), 890-902. doi:10.1016/j.chembiol.2014.06.003

Schroeder, B. C., Cheng, T., Jan, Y. N., & Jan, L. Y. (2008). Expression cloning of TMEM16A as a calcium-activated chloride channel subunit. *Cell, 134*(6), 1019-1029. doi:10.1016/j.cell.2008.09.003

Scott, S. A., Selvy, P. E., Buck, J. R., Cho, H. P., Criswell, T. L., Thomas, A. L., . . . Brown, H. A. (2009). Design of isoform-selective phospholipase D inhibitors that modulate cancer cell invasiveness. *Nat Chem Biol, 5*(2), 108-117. doi:10.1038/nchembio.140

Session, A. M., Uno, Y., Kwon, T., Chapman, J. A., Toyoda, A., Takahashi, S., . . . Rokhsar, D. S. (2016). Genome evolution in the allotetraploid frog Xenopus laevis. *Nature, 538*(7625), 336-343. doi:10.1038/nature19840

Singer, A. U., Waldo, G. L., Harden, T. K., & Sondek, J. (2002). A unique fold of phospholipase C-beta mediates dimerization and interaction with G alpha q. *Nat Struct Biol, 9*(1), 32-36. doi:10.1038/nsb731

Skinner, M. K. (2018). *Encyclopedia of reproduction* (Second edition. ed.). Amsterdam ; Boston: Elsevier, Academic Press.

Smrcka, A. V., Hepler, J. R., Brown, K. O., & Sternweis, P. C. (1991). Regulation of polyphosphoinositide-specific phospholipase C activity by purified Gq. *Science, 251*(4995), 804-807. doi:10.1126/science.1846707

Spallanzani, L., Bonnet, C., & Beddoes, T. (1789). *Dissertations relative to the natural history of animals and vegetables* (A new edition corrected and enlarged ... ed.). London: Printed for J. Murray.

Stallings, J. D., Tall, E. G., Pentyala, S., & Rebecchi, M. J. (2005). Nuclear translocation of phospholipase C-delta1 is linked to the cell cycle and nuclear phosphatidylinositol 4,5-bisphosphate. *J Biol Chem, 280*(23), 22060-22069. doi:10.1074/jbc.M413813200

Steinhardt, R. A., Lundin, L., & Mazia, D. (1971). Bioelectric responses of the echinoderm egg to fertilization. *Proc Natl Acad Sci U S A, 68*(10), 2426-2430. doi:10.1073/pnas.68.10.2426

Stith, B. J. (2015). Phospholipase C and D regulation of Src, calcium release and membrane fusion during Xenopus laevis development. *Dev Biol, 401*(2), 188-205. doi:10.1016/j.ydbio.2015.02.020

Stricker, S. A. (1999). Comparative biology of calcium signaling during fertilization and egg activation in animals. *Dev Biol, 211*(2), 157-176. doi:10.1006/dbio.1999.9340

Su, W., Yeku, O., Olepu, S., Genna, A., Park, J. S., Ren, H., . . . Frohman, M. A. (2009). 5-Fluoro-2-indolyl des-chlorohalopemide (FIPI), a phospholipase D pharmacological inhibitor that alters cell spreading and inhibits chemotaxis. *Mol Pharmacol, 75*(3), 437-446. doi:10.1124/mol.108.053298

Sugiyama, H., Burnett, L., Xiang, X., Olson, J., Willis, S., Miao, A., . . . Chandler, D. E. (2009). Purification and multimer formation of allurin, a sperm chemoattractant from Xenopus laevis egg jelly. *Mol Reprod Dev, 76*(6), 527-536. doi:10.1002/mrd.20969

Tembo, M., Bainbridge, R. E., Lara-Santos, C., Komondor, K. M., Daskivich, G. J., Durrant, J. D., . . . Carlson, A. E. (2022). Phosphate position is key in mediating transmembrane ion channel TMEM16A-phosphatidylinositol 4,5-bisphosphate interaction. *J Biol Chem, 298*(8), 102264. doi:10.1016/j.jbc.2022.102264

Tembo, M., Sauer, M. L., Wisner, B. W., Beleny, D. O., Napolitano, M. A., & Carlson, A. E. (2021). Actin polymerization is not required for the fast block to polyspermy in the African clawed frog, Xenopus laevis. *MicroPubl Biol, 2021*. doi:10.17912/micropub.biology.000365

Teves, M. E., Guidobaldi, H. A., Unates, D. R., Sanchez, R., Miska, W., Publicover, S. J., . . . Giojalas, L. C. (2009). Molecular mechanism for human sperm chemotaxis mediated by progesterone. *PLoS One, 4*(12), e8211. doi:10.1371/journal.pone.0008211

Tholl, N., Naqvi, S., McLaughlin, E., Boyles, S., Bieber, A. L., & Chandler, D. E. (2011). Swimming of Xenopus laevis sperm exhibits multiple gears and its duration is extended by egg jelly constituents. *Biol Bull, 220*(3), 174-185. doi:10.1086/BBLv220n3p174

Tian, J., Gong, H., Thomsen, G. H., & Lennarz, W. J. (1997). Gamete interactions in Xenopus laevis: identification of sperm binding glycoproteins in the egg vitelline envelope. *J Cell Biol, 136*(5), 1099-1108. doi:10.1083/jcb.136.5.1099

Tokmakov, A. A., Sato, K. I., Iwasaki, T., & Fukami, Y. (2002). Src kinase induces calcium release in Xenopus egg extracts via PLCgamma and IP3-dependent mechanism. *Cell Calcium, 32*(1), 11-20. doi:10.1016/s0143-4160(02)00078-7

Tokmakov, A. A., Stefanov, V. E., Iwasaki, T., Sato, K., & Fukami, Y. (2014). Calcium signaling and meiotic exit at fertilization in Xenopus egg. *Int J Mol Sci, 15*(10), 18659-18676. doi:10.3390/ijms151018659

Touhara, K. K., & MacKinnon, R. (2018). Molecular basis of signaling specificity between GIRK channels and GPCRs. *Elife, 7*. doi:10.7554/eLife.42908

Uemura, T., Kawasaki, T., Taniguchi, M., Moritani, Y., Hayashi, K., Saito, T., . . . Miyata, K. (2006). Biological properties of a specific Galpha q/11 inhibitor, YM-254890, on platelet functions and thrombus formation under high-shear stress. *Br J Pharmacol, 148*(1), 61-69. doi:10.1038/sj.bjp.0706711

Unsicker, K., Axelsson, S., Owman, C., & Svensson, K. G. (1975). Innervation of the male genital tract and kidney in the amphibia, Xenopus laevis Daudin, Rana temporaria L., and Bufo bufo L. *Cell Tissue Res, 160*(4), 453-484. doi:10.1007/BF00225764

Wagner, J., Li, Y. X., Pearson, J., & Keizer, J. (1998). Simulation of the fertilization Ca2+ wave in Xenopus laevis eggs. *Biophys J, 75*(4), 2088-2097. doi:10.1016/S0006-3495(98)77651-9

Wahl, M. I., Jones, G. A., Nishibe, S., Rhee, S. G., & Carpenter, G. (1992). Growth factor stimulation of phospholipase C-gamma 1 activity. Comparative properties of control and activated enzymes. *J Biol Chem, 267*(15), 10447-10456. Retrieved from https://www.ncbi.nlm.nih.gov/pubmed/1316902

Watabe, M., Izaki, K., Fujino, S., Maruyama, M., Kojima, C., Hiraiwa, A., . . . Iwao, Y. (2019). The electrical block to polyspermy induced by an intracellular Ca(2+) increase at fertilization of the clawed frogs, Xenopus laevis and Xenopus tropicalis. *Mol Reprod Dev, 86*(4), 387-403. doi:10.1002/mrd.23115

Webb, D. J., & Nuccitelli, R. (1985). Fertilization potential and electrical properties of the Xenopus laevis egg. *Dev Biol, 107*(2), 395-406. doi:10.1016/0012-1606(85)90321-5

Wessel, G. M., & Wong, J. L. (2009). Cell surface changes in the egg at fertilization. *Mol Reprod Dev, 76*(10), 942-953. doi:10.1002/mrd.21090

Whitaker, M. (2006). Calcium at fertilization and in early development. *Physiol Rev, 86*(1), 25-88. doi:10.1152/physrev.00023.2005

Whitaker, M. J., & Steinhardt, R. A. (1983). Evidence in support of the hypothesis of an electrically mediated fast block to polyspermy in sea urchin eggs. *Dev Biol, 95*(1), 244-248. doi:10.1016/0012-1606(83)90024-6

Wing, M. R., Bourdon, D. M., & Harden, T. K. (2003). PLC-epsilon: a shared effector protein in Ras-, Rho-, and G alpha beta gamma-mediated signaling. *Mol Interv, 3*(5), 273-280. doi:10.1124/mi.3.5.273

Wing, M. R., Houston, D., Kelley, G. G., Der, C. J., Siderovski, D. P., & Harden, T. K. (2001). Activation of phospholipase C-epsilon by heterotrimeric G protein betagamma-subunits. *J Biol Chem, 276*(51), 48257-48261. doi:10.1074/jbc.C100574200

Wing, M. R., Snyder, J. T., Sondek, J., & Harden, T. K. (2003). Direct activation of phospholipase C-epsilon by Rho. *J Biol Chem, 278*(42), 41253-41258. doi:10.1074/jbc.M306904200

Wong, J. L., & Wessel, G. M. (2006). Defending the zygote: search for the ancestral animal block to polyspermy. *Curr Top Dev Biol, 72*, 1-151. doi:10.1016/S0070-2153(05)72001-9

Wozniak, K. L., Bainbridge, R. E., Summerville, D. W., Tembo, M., Phelps, W. A., Sauer, M. L., . . . Carlson, A. E. (2020). Zinc protection of fertilized eggs is an ancient feature of sexual reproduction in animals. *PLoS Biol, 18*(7), e3000811. doi:10.1371/journal.pbio.3000811

Wozniak, K. L., Mayfield, B. L., Duray, A. M., Tembo, M., Beleny, D. O., Napolitano, M. A., . . . Carlson, A. E. (2017). Extracellular Ca2+ Is Required for Fertilization in the African Clawed Frog, Xenopus laevis. *PLoS One, 12*(1), e0170405. doi:10.1371/journal.pone.0170405

Wozniak, K. L., Phelps, W. A., Tembo, M., Lee, M. T., & Carlson, A. E. (2018). The TMEM16A channel mediates the fast polyspermy block in Xenopus laevis. *J Gen Physiol, 150*(9), 1249-1259. doi:10.1085/jgp.201812071

Wozniak, K. L., Tembo, M., Phelps, W. A., Lee, M. T., & Carlson, A. E. (2018). PLC and IP3-evoked Ca(2+) release initiate the fast block to polyspermy in Xenopus laevis eggs. *J Gen Physiol, 150*(9), 1239-1248. doi:10.1085/jgp.201812069

Wright, E. M., & Diamond, J. M. (1977). Anion selectivity in biological systems. *Physiol Rev, 57*(1), 109-156. doi:10.1152/physrev.1977.57.1.109

Wuhr, M., Freeman, R. M., Jr., Presler, M., Horb, M. E., Peshkin, L., Gygi, S., & Kirschner, M. W. (2014). Deep proteomics of the Xenopus laevis egg using an mRNA-derived reference database. *Curr Biol, 24*(13), 1467-1475. doi:10.1016/j.cub.2014.05.044

Wymann, M. P., Bulgarelli-Leva, G., Zvelebil, M. J., Pirola, L., Vanhaesebroeck, B., Waterfield, M. D., & Panayotou, G. (1996). Wortmannin inactivates phosphoinositide 3-kinase by covalent modification of Lys-802, a residue involved in the phosphate transfer reaction. *Mol Cell Biol, 16*(4), 1722-1733. doi:10.1128/MCB.16.4.1722

Wyrick, R. E., Nishihara, T., & Hedrick, J. L. (1974). Agglutination of jelly coat and cortical granule components and the block to polyspermy in the amphibian Xenopus laevis. *Proc Natl Acad Sci U S A, 71*(5), 2067-2071. doi:10.1073/pnas.71.5.2067

Xiang, X., Burnett, L., Rawls, A., Bieber, A., & Chandler, D. (2004). The sperm chemoattractant "allurin" is expressed and secreted from the Xenopus oviduct in a hormone-regulated manner. *Dev Biol, 275*(2), 343-355. doi:10.1016/j.ydbio.2004.08.011

Yang, J., Aguero, T., & King, M. L. (2015). The Xenopus Maternal-to-Zygotic Transition from the Perspective of the Germline. *Curr Top Dev Biol, 113*, 271-303. doi:10.1016/bs.ctdb.2015.07.021

Zhou, Y., Sondek, J., & Harden, T. K. (2008). Activation of human phospholipase C-eta2 by Gbetagamma. *Biochemistry, 47*(15), 4410-4417. doi:10.1021/bi800044n

Zhou, Y., Wing, M. R., Sondek, J., & Harden, T. K. (2005). Molecular cloning and characterization of PLC-eta2. *Biochem J, 391*(Pt 3), 667-676. doi:10.1042/BJ20050839